

**One Dimensional Analysis Model of a
Condensing Spray Chamber Including Rocket Exhaust
Using SINDA/FLUINT and CEA**

**Barbara A. Sakowski
Daryl Edwards
Kevin Dickens**

NASA Glenn Research Center

August, 2014

Table of Contents

Introduction.....	4
Facility and Exhaust System Description	4
Model Description	7
Model Details: Submodel “A”	11
SINDA/FLUINT Modeling of Supersonic Flow	11
CEA Modeling Applications.....	13
Duct Wall Cooling.....	15
Transient Control	16
Model Details: Submodel “B”	16
Model Setup.....	16
Droplet Model: Momentum	20
Droplet Model: Heat Transfer.....	23
Droplet Model: Heat Transfer Applied in SINDA/FLUINT	27
Model Details: Submodel “C”	30
Model Setup.....	30
Results.....	32
Appendix A: CEA and SINDA/FLUINT Enthalpy and Entropy Reference States.....	38
Appendix B: Calculation of Droplet Inlet Velocity from the Condenser Spray Bar	43
Appendix C: Abbreviations and Acronyms.....	44
References.....	49

Table of Figures

Figure 1: Aerial View of Spacecraft Propulsion Research Facility (B-2)	5
Figure 2: Cutaway view of the B-2 test building.....	6
Figure 3: Condensing Spray System.....	7
Figure 4: B2 Facility	8
Figure 5: SINDA/FLUINT Submodel “A” of Rocket Exhaust Duct	10
Figure 6: FLUINT Submodel “B” of Spray Chamber	10
Figure 7: SINDA Submodel “C” of Droplet.....	11
Figure 8: FLUINT Model Setup of Spray Chamber.....	18
Figure 9: FLUINT Model Setup of Spray Chamber.....	19
Figure 10: Characteristic Droplet in FLUINT Stratified Tank or “Pancake”	21
Figure 11: Forces Acting on a Droplet	21
The forces acting on the droplet are illustrated in.....	21
Figure 10 and	Error! Bookmark not defined.
Figure 12: Heat Transfer Mechanisms between Exhaust Duct Flow and Droplet	23
Figure 13: Summary Table of Delta III Upper Stage Hot Fire Tests.....	32
Figure 14: Spray Chamber Pressure for Hotfire Test 3 and SINDA/FLUINT Model Results.....	33
Figure 15: Spray Chamber Pressure for Hotfire Test 6 and SINDA/FLUINT Model Results.....	33
Figure 16: Spray Chamber Pressure for Hotfire Test 8 and SINDA/FLUINT Model Results.....	34

Figure 17: Spray Chamber Pressure for Hotfire Test 10 and SINDA/FLUINT Model Results..... 34

Figure 18: Summary Table of Candidate Test Article Input 35

Figure 19: Spray Chamber Pressure for Candidate Test Article SINDA/FLUINT Model Results..... 35

Figure 20: Spray Chamber Spray Water Temperature for Candidate Test Article SINDA/FLUINT Model Results..... 36

Introduction

Modeling droplet condensation via CFD codes can be very tedious, time consuming, and inaccurate. CFD codes may be tedious and time consuming in terms of using Lagrangian particle tracking approaches or particle sizing bins. Also since many codes ignore conduction through the droplet and or the degrading effect of heat and mass transfer if noncondensable species are present, the solutions may be inaccurate. The modeling of a condensing spray chamber where the significant size of the water droplets and the time and distance these droplets take to fall, can make the effect of droplet conduction a physical factor that needs to be considered in the model. Furthermore the presence of even a relatively small amount of noncondensable has been shown to reduce the amount of condensation [Ref 1]. It is desirable then to create a modeling tool that addresses these issues. The path taken to create such a tool is illustrated. The application of this tool and subsequent results are based on the spray chamber in the Spacecraft Propulsion Research Facility (B2) located at NASA's Plum Brook Station that tested an RL-10 engine. The platform upon which the condensation physics is modeled is SINDA/FLUINT. The use of SINDA/FLUINT enables the ability to model various aspects of the entire testing facility, including the rocket exhaust duct flow and heat transfer to the exhaust duct wall. The ejector pumping system of the spray chamber is also easily implemented via SINDA/FLUINT. The goal is to create a transient one dimensional flow and heat transfer model beginning at the rocket, continuing through the condensing spray chamber, and finally ending with the ejector pumping system. However the model of the condensing spray chamber may be run independently of the rocket and ejector systems detail, with only appropriate mass flow boundary conditions placed at the entrance and exit of the condensing spray chamber model. The model of the condensing spray chamber takes into account droplet conduction as well as the degrading effect of mass and heat transfer due to the presence of noncondensibles. The one dimensional model of the condensing spray chamber makes no presupposition on the pressure profile within the chamber, allowing the implemented droplet physics of heat and mass transfer coupled to the SINDA/FLUINT solver to determine a transient pressure profile of the condensing spray chamber. Model results compare well to the RL-10 engine pressure test data.

Facility and Exhaust System Description

A brief description of the facility and its exhaust system is included in this section. Figure 1 is an aerial view of the Plum Brook Station B-2 test facility.



Figure 1: Aerial View of Spacecraft Propulsion Research Facility (B-2)

Constructed in the 1960s, primarily to support the Centaur upper stage development, the Spacecraft Propulsion Research Facility (B-2) provides the facilities to simulate a space thermal soak and subsequent altitude firing of the propulsion system. Testing can consist of a variety of combinations including engine only, engine plus propellant delivery systems, or an integrated stage incorporating tanks and avionics. The facility is equipped with propellant delivery systems for LOX and LH2 plus helium and nitrogen supporting systems and is sized for hydrogen-oxygen engines up to 445 kN (100,000 lbf) thrust and approximately 200 kN (45,000 lbf) thrust for storable (non-condensable) propellant combinations.

Space simulation is accomplished in a stainless steel cylindrical vacuum chamber 11.6 meter (38 feet) diameter with a 18.9 meters (62 feet) vertical height. Vacuum pumping includes 3 stages of mechanical pumps and ten diffusion pumps ultimately bringing the vacuum chamber to a 10^{-4} Pa (10^{-5} Pa with liquid nitrogen in the cold wall) environment for well sealed systems. Thermal simulation is provided on the cold end by a liquid nitrogen cold wall and on the high end by portable lamps configured as required for the test.

Engine firing is accomplished by opening a 3.4 meter (11 ft) diameter valve [located at the end of the 12 meter (39 ft) diffuser] allowing the exhaust products to enter a spray chamber which cools and condenses the exhaust through circulation of 848 kL/min (224,000 gpm) of spray water from the water stored in the spray chamber. The 20.4 meter (67 ft) diameter by 36 meter (118 ft) deep concrete spray chamber is pumped by a steam ejector system to transport the remaining exhaust products to the atmosphere.

To maintain vacuum conditions during engine firing, it is necessary to remove the products of combustion as fast as they are generated. At B-2, this is accomplished by a spray condensing system designed to condense steam (a product of combustion for hydrogen-oxygen engines) and an ejector system to pump out non-condensable gases

such as excess hydrogen. The ejectors are visible in the aerial view immediately to the right of the test building.

Figure 2 is a cut-away view of the test building. A basic understanding can be made from this view as it shows a rocket upper stage (containing two engines) being lowered into the test chamber. Located immediately below the test chamber is the spray chamber where the rocket's exhaust is exposed to water sprays (which condense a portion of the exhaust) as illustrated in Figure 3. Excess exhaust water vapor and the non-condensable gases are then removed by the primary ejector system which is powered by the steam supply system. The primary ejector system consists of 2 parallel trains with each train having 3-stages of ejectors. A quick observation reveals that much of the exhaust system's function occurs below ground.

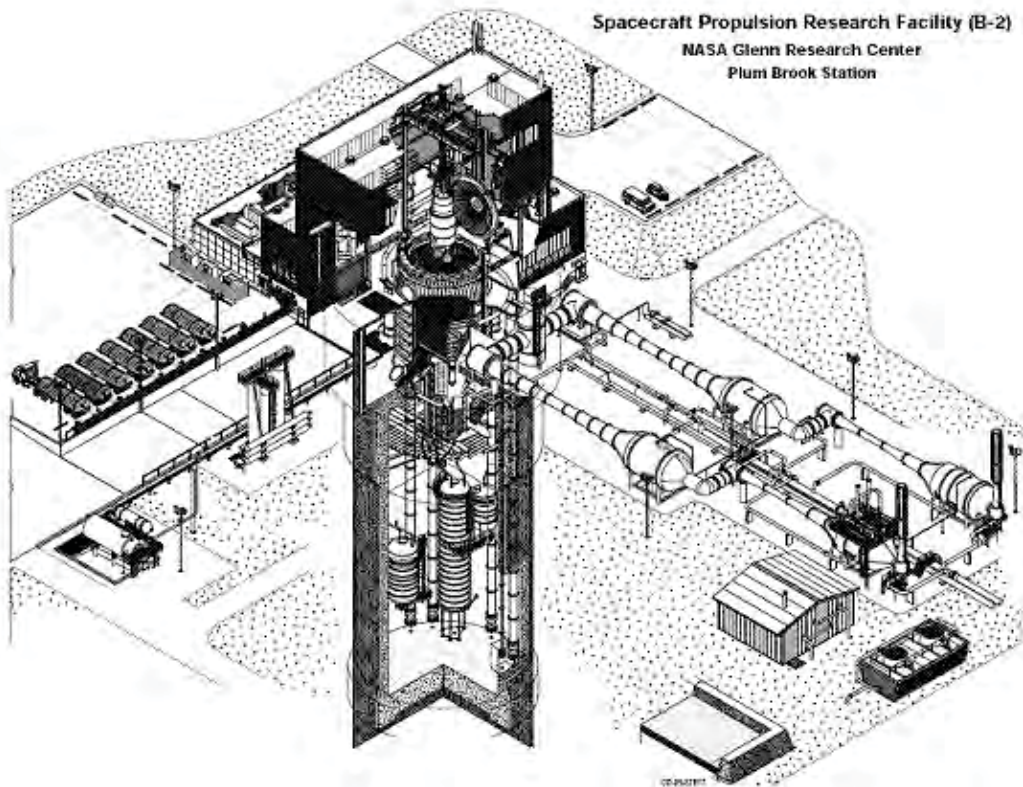


Figure 2: Cutaway view of the B-2 test building

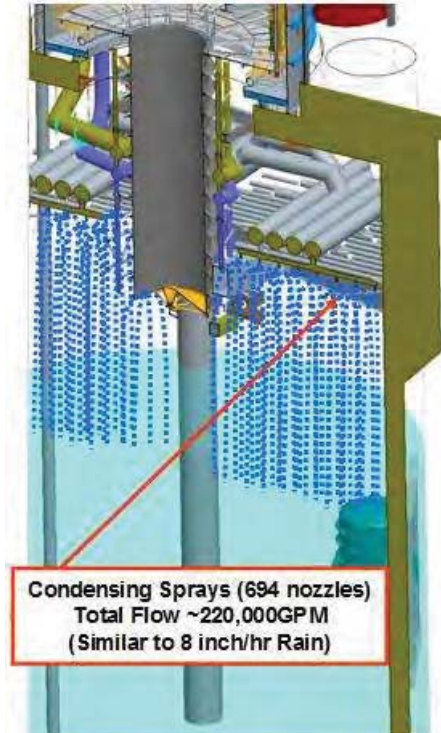


Figure 3: Condensing Spray System

An important point to make is that as the test engines get larger and generate more products of combustion into the spray chamber, there will be some point where the spray chamber cannot condense enough of the rocket generated steam to maintain the low spray chamber pressures. The excess water vapor will start loading up the ejectors to the point where they cannot keep up. The spray chamber pressure will then begin a rapid pressure growth causing conditions at the engine to no longer satisfy test requirements.

Model Description

SINDA/FLUINT is used as the platform to model the rocket exhaust duct and spray chamber of the B2 facility. A schematic of the facility is shown in Figure 4.

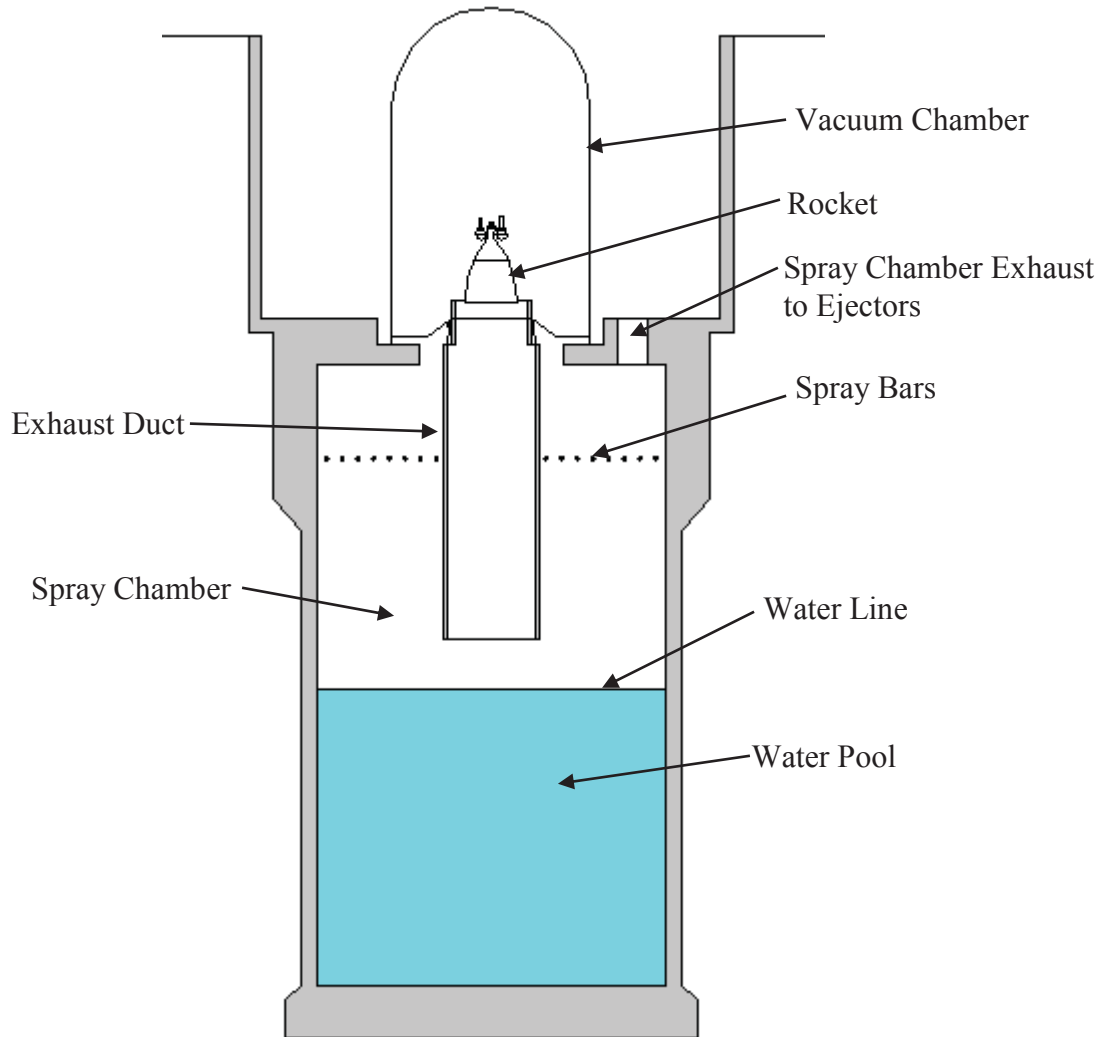


Figure 4: B2 Facility

The rocket exhaust is modeled using the Chemical Equilibrium with Applications code (CEA). CEA is included as a subroutine in the SINDA/FLUINT model and is therefore called from within the SINDA/FLUINT input file. The model is setup in a parametric manner so that all input, including CEA input, is set through the Register Data in SINDA/FLUINT. The input in the Register Data may also be input via an Excel Spreadsheet instead of through the ASCII SINDA/FLUINT input file. The expanded flow exiting the rocket, modeled in CEA, is input to the SINDA/FLUINT model of the rocket exhaust duct. The rocket exhaust duct flow is modeled using the FLUINT portion of SINDA/FLUINT (the fluids system analyzer) and the rocket duct wall is modeled in SINDA (the thermal analyzer). Thus heat transfer to the wall including any water spray used to cool the exterior of the duct wall may be modeled. The geometry of the rocket exhaust duct may be input in a simplified “lumped” approach or through more sophisticated methods, (i.e., full 3-D geometries). Currently the model has the ability to interface with MSC.Patran. The geometry can be built in MSC Patran, imported into SINDA/FLUINT, and then the thermal results can be mapped back on to the 3-D MSC Patran model.

Figure 5 through Figure 7 qualitatively illustrate the numerical model of the B2 facility as represented in SINDA/FLUINT. The model is composed of three primary submodels, “A”, “B”, “C”. Figure 5 illustrates Submodel “A”, which models the combined rocket duct flow and rocket duct wall model as described above. This submodel utilizes CEA to initialize the flow into the duct. Although Figure 5 illustrates fluid convection of the rocket duct flow and the rocket duct wall thermal conduction only in the radial direction, the wall geometry may include axial conduction as well. The MSC Patran model incorporates 3-D conduction through the rocket exhaust duct wall.

At the end of the rocket exhaust duct CEA is called once more to calculate the shocked flow conditions. CEA is also used to model the quenching of the shocked flow. The quenched flow conditions are used as input to the spray chamber Submodel “B” of SINDA/FLUINT. The user may elect to run the SINDA/FLUINT model with only the rocket exhaust duct Submodel “A” and not with the spray chamber Submodel “B”. The shocking and quenching of the flow is contained in Submodel “A”, and updated in Submodel “B”.

Figure 6 illustrates Submodel “B” which uses the shocked and quenched flow from Submodel “A” as input flow conditions to the spray chamber. The entrance location of the inflow is assumed to be at the bottom of the spray chamber which is also the location of the water line. The spray chamber is modeled in FLUINT as a stratified vessel or a series of stacked “pancakes” that pass flow in one direction (upwards in Figure 56). The outflow of the spray chamber employs an ejector pump curve as a function tank pressure. The condensing spray flow dynamics and heat transfer is modeled via user FORTRAN and is based on particle flow mechanics.

Figure 7 illustrates the thermal model of a single characteristic droplet that resides at a given time in a “pancake” as modeled in SINDA. The heat rate on the particle is determined through user FORTRAN via a heat transfer coefficient which relates the thermal environment of its respective “pancake” determined by FLUINT and the droplet wall temperature determined by SINDA. The conduction through the droplet can be discretized to any number of “n” nodes. A radial conductor, “G_n”, may be determined via the following:

Eq. 1
$$G_n = 4\pi k_d \frac{r_n r_{n-1}}{r_{n-1} - r_{n-1}} \quad [W/K]$$

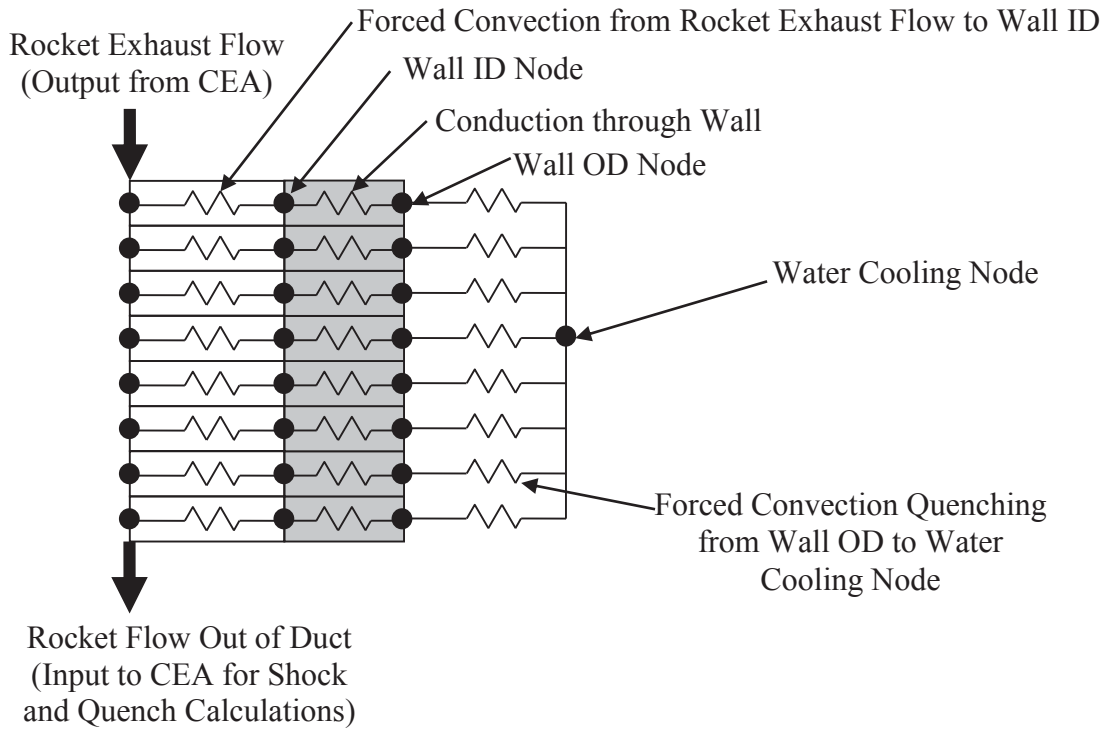


Figure 5: SINDA/FLUINT Submodel “A” of Rocket Exhaust Duct

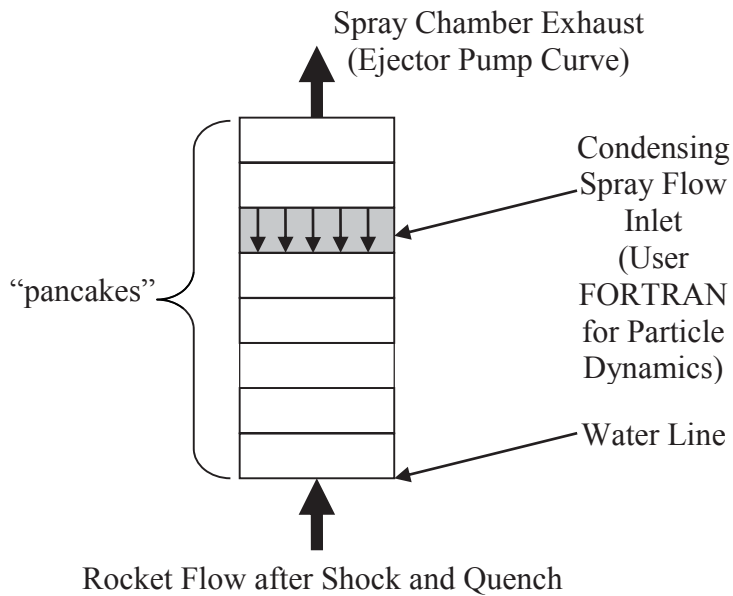


Figure 6: FLUINT Submodel “B” of Spray Chamber

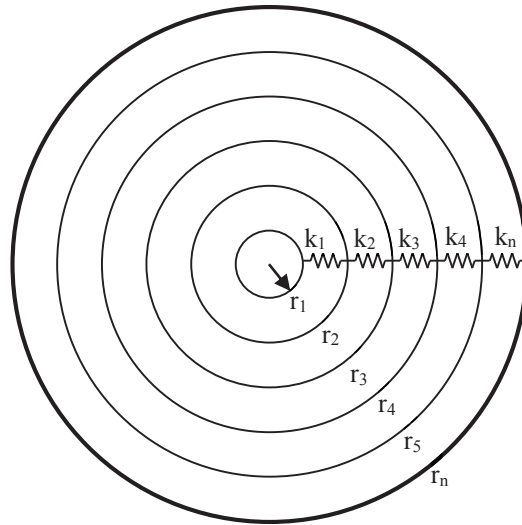


Figure 7: SINDA Submodel “C” of Droplet

It should be noted that Submodel “B” is inherently built as a true transient thereby making Submodel “C” also a true transient. This is because the “pancakes” illustrated in Figure 4Figure 6 are modeled in FLUENT as tanks which inherently have volume and therefore mass. The submodel’s physics require the use of these parameters. Submodel “A” however runs with the steady state solver but can be run as a “false” transient with a series of steady state runs.

Model Details: Submodel “A”

The SINDA/FLUENT Submodel “A” models the rocket duct flow and heat transfer through the rocket duct wall. The submodel also utilizes CEA to initialize the rocket duct flow, shock the exit duct flow, and quench the exit duct flow with cooling water. CEA is run within SINDA/FLUENT as a subroutine. Other applications of CEA will be outlined below as well as in the section, **CEA Modeling Applications.**

SINDA/FLUENT Modeling of Supersonic Flow

The rocket exhaust duct flow or duct entrance flow is supersonic. In order for SINDA/FLUENT to model supersonic flow several modeling techniques are employed. There are five significant issues that need to be addressed. These issues regard the use of FLUENT. First, a FLUENT set mass flow rate connector (MFRSET), is placed at the duct exit. Second, all choking calculations must be turned off in FLUENT. Third, set IPDC=0 for the FLUENT connectors, i.e., duct friction calculations are supplied by the user. This is necessary for several reasons. Fluid properties used in the calculation of the friction factor must be evaluated at a reference temperature because of the extreme temperature variations which are produced in the compressible boundary layer. Currently, FLUENT does not evaluate fluid properties at a reference temperature in calculating friction factors. Equation 2 is used to evaluate fluid properties in calculating the friction factor [Ref 2]:

$$\text{Eq. 2} \quad T_{\text{ref}} = 0.5(T_{\text{wall}} + T_{\text{fluid}}) + 0.22(T_{\text{rec}} - T_{\text{stat}}) \quad [\text{K}]$$

The recovery temperature is defined by [Ref 3]:

$$\text{Eq. 3} \quad T_{\text{rec}} = \text{Pr}^{1/3} (T_{\text{stag}} - T_{\text{stat}}) + T_{\text{stat}} \quad [\text{K}]$$

In order for FLUENT to obtain a stable supersonic solution, the friction factor must be input as a *positive* “FC” value with an “FPOW” exponent equal to one. Normally the “FC” value is negative. A negative value causes FLUENT’s solver to pursue a subsonic solution. The friction factor for flow through a duct with fluid properties evaluated at T_{ref} is given by [Ref 3]:

$$\text{Eq. 4} \quad F = 0.184 \text{Re}^{-0.2} \frac{L_D}{D_D}$$

The FLUENT “FC” factor can then be updated through user logic via the equation [Ref 4]:

$$\text{Eq. 5} \quad \text{FC} = \frac{F}{2\text{Ac}_D^2 \rho} \quad [1/\text{m}^2/\text{kg}]$$

It is important to note that in using this procedure to obtain a supersonic solution, that the DUCT MACRO option in FLUENT should not be used. This is because this macro automatically imposes an AC factor which is not appropriate for this case. Equivalent results can also be obtained by imposing a negative FK factor, the negative of Equation 4, or imposing a positive HC factor (pressure gain), Equation 5 multiplied by the mass flow rate squared.

The fourth issue regarding supersonic flow involves heat transfer. The heat transfer to the duct wall is also supplied via user logic. A turbulent heat transfer coefficient is calculated with fluid properties evaluated at T_{ref} using the Colburn Analogy [Ref 3]:

$$\text{Eq. 6} \quad h_D = 0.23 \text{Re}^{0.8} \text{Pr}^{1/3} \frac{k}{D_D} \quad [\text{W}/\text{m}^2/\text{K}]$$

Since the convecting fluid temperature to the duct wall should be the recovery temperature, Eq. 2, and not the static temperature the following modeling techniques are employed. Thermal boundary nodes that analogously represent the fluid lumps in the duct are created. They are updated in user logic to correspond to the respective recovery temperature of the fluid lump. Thermal conductors are created from these thermal boundary nodes to the duct wall nodes. These conductors are updated in user logic using Eq. 6. The heat rate leaving a fluid lump and going into the respective duct wall node can be calculated using Eq 6:

$$\text{Eq. 7} \quad Q_D = h_D A_{SD} (T_{\text{rec}} - T_{\text{wall}}) \quad [\text{W}]$$

It should be noted that FLUINT does have a utility that incorporates a reference temperature in heat transfer calculations. The above procedure just illustrates an alternative approach.

Finally, the fifth issue regarding FLUINT and supersonic flow is not trivial. Currently FLUINT imposes a velocity limit on the kinetic energy term in the total enthalpy energy equation for stability reasons. This limit does not allow for the maximum velocity attained in the supersonic flow modeled in the analysis of the B2 facility. The mach numbers calculated in the analysis of the B2 facility ranged from 0.0 to 8.0. For the exact velocity limit used in FLUINT, Cullimore & Ring Technologies should be consulted for this value may depend on the version of SINDA/FLUINT being used. The FLUINT maximum velocity constraint in this analysis was 3000 m/s. This constraint did not allow for the conservation of total enthalpy for adiabatic flow. In order to “conserve” total enthalpy a heat rate was imposed on the fluid lumps representing the duct flow. This heat rate represented the “pseudo” kinetic energy term that was missing because of the velocity limit. The heat rates for the individual fluid lumps were calculated in user logic so that the total enthalpies for the respective lumps were conserved. This process was also repeated for flow that included heat transfer to the wall. The entire process for determining the “pseudo” heat rates involved several SINDA/FLUINT FASTIC calls (i.e., steady state calls). First a steady state solution is obtained for the duct flow with no wall heat transfer and no imposed “pseudo” kinetic energy heat rates. This yields a solution that does not conserve total enthalpy. A second steady state call is then made that employs user logic to calculate the necessary heat rates to conserve total enthalpy for the individual fluid lumps. This second run restarts from the results of the first run. If wall heat transfer is modeled, a third steady state call is made that restarts from the results of the second steady state run. This third steady state call recalculates new “pseudo” heat rates that take into account the heat rate to the wall.

In order to execute the aforementioned procedure, the stagnation conditions of the duct flow fluid lumps must be calculated. For no wall heat transfer this calculation need only be executed once since stagnation enthalpy is conserved. However for the case of wall heat transfer each fluid lump will have a new stagnation state. The problem in calculating stagnation conditions lies in that most property tables do not go to such high temperature conditions. One way to circumvent this is to use CEA to calculate stagnation conditions.

CEA Modeling Applications

CEA, Chemical Equilibrium with Applications, is a NASA developed code that calculates mixture chemical equilibrium compositions and properties. The source code is written in ANSI standard FORTRAN, and is appended as a subroutine to the SINDA/FLUINT model of the B2 facility. CEA is used for several functions in the

model. First, CEA determines the rocket exhaust duct flow properties that serve as inlet conditions to the rocket duct SINDA/FLUINT model. The rocket setup in CEA is run as an enthalpy/pressure case. For a given area ratio, CEA outputs parameters that can be used to calculate the rocket duct mass flow rate. The mass flow rate, pressure, and temperature output from CEA, for a given area ratio, are used as input to the SINDA/FLUINT rocket duct model. This is accomplished via user logic.

CEA is also used to determine duct flow stagnation properties. For a given fluid lump where pressure, temperature, enthalpy, and entropy are known via SINDA/FLUINT, CEA may be used to determine the stagnation conditions of the fluid lump. A subroutine was created that sets up a CEA run and is called from user logic. The user may elect to send this subroutine the enthalpy, entropy, and pressure of a given fluid lump, determined via SINDA/FLUINT, or the user may elect to send the temperature and pressure of a given fluid lump, determined via SINDA/FLUINT. If temperature and pressure values are selected to be sent to the subroutine, then the subroutine first calls a temperature/pressure case in CEA so that the enthalpy and entropy may be determined. Also required as input to this subroutine, is the flow velocity associated with the fluid lump. Given the velocity and pressure of the fluid lump, a “guessed” value of the total pressure is calculated. The velocity and enthalpy, either supplied by SINDA/FLUINT or calculated via CEA, is used to calculate the total enthalpy of the fluid lump. The value of total pressure is used to run an entropy/pressure case in CEA. The output enthalpy calculated via CEA is then compared to the total enthalpy calculated from the user inputs of enthalpy and velocity. If these two values are not converged, a new guess on the total pressure is calculated and the procedure is repeated. Upon convergence, the subroutine returns total conditions of the fluid lump, (i.e., temperature, pressure and enthalpy).

Another subroutine was created that sets up a CEA shock run. This subroutine is called from user logic in SINDA/FLUINT, using the fluid properties of the exit fluid lump in the rocket duct. For a given fluid lump where pressure and temperature are known via SINDA/FLUINT, as well as the velocity associated with the fluid lump, CEA calculates the post-shock flow properties.

The properties of the shocked flow are used in the quench calculations. This shocked rocket duct flow exhaust is quenched with cooling water that runs along the outside of the rocket duct. Another subroutine utilizing CEA was created to calculate the quench water flow rate needed to bring the shocked rocket duct flow exhaust to the inlet quench cooling water temperature at the spray chamber pressure. Ultimately this is a transient process since the spray chamber pressure varies as a function of time. The total enthalpy of the shocked rocket exhaust duct flow, calculated using the aforementioned subroutine, as well as the enthalpy of the quenched cooling water, supplied via SINDA/FLUINT, is sent to this subroutine. It should be noted that the subcooling of the quenched cooling water is taken into account in the SINDA/FLUINT water property database. This subroutine sets up an iterative enthalpy/pressure calling procedure to CEA that guesses an initial mass flow rate of the quench cooling water. The enthalpy that is sent to CEA in this enthalpy/pressure procedure is defined by:

$$\text{Eq. 8} \quad H_{\text{quench}} = \frac{\dot{m}_{\text{duct}} H_{\text{duct}} + \dot{m}_{\text{water}} H_{\text{water}}}{\dot{m}_{\text{water}} + \dot{m}_{\text{duct}}} \quad [\text{J/kg}]$$

The mass flow rate of the quench cooling water is iterated upon until the temperature of the vapor mixture, calculated by CEA, converges to the inlet quench cooling temperature. If the mass flow rate of the quench cooling water is less than the total inlet quench cooling water mass flow rate, the excess water is removed from the system (i.e., the water pool, see Figure 4). This quenched vapor serves as the inlet conditions to the spray chamber model, Submodel “B”.

A final note regarding CEA and SINDA/FLUINT needs to be addressed. Many of the SINDA/FLUINT property databases are generated with REFPROP, Reference Fluid Thermodynamic and Transport Properties. This is a NIST standard reference database [Ref 5]. Care needs to be taken in transferring enthalpy and entropy values between CEA [Ref 6], and SINDA/FLUINT because the reference states used by each code may not coincide. Please refer to Appendix A for more information.

Duct Wall Cooling

The outside of the rocket duct is cooled by the quench cooling water. The quench cooling water is maintained at the spray chamber pressure and the inlet condenser spray temperature. A heat transfer coefficient is calculated that includes film boiling and convection. The film boiling heat transfer coefficient, which takes into account subcooling of the water, is given by [Ref 7]:

$$\text{Eq. 9} \quad h_{\text{film}} = 0.62 \left(\frac{k_v^3 g \rho_v (\rho_l - \rho_v) h'_{\text{fg}}}{\mu_v D o_{\text{duct}} (T o_{\text{duct}} - T_{\text{sat}})} \right)^{0.25} \quad [\text{W/m}^2/\text{K}]$$

where

$$\text{Eq. 10} \quad h'_{\text{fg}} = (1.0 + 0.68 \text{ Ja}) h_{\text{fg}} \quad [\text{J/kg/K}]$$

and Ja is the Jakob number.

The forced convection heat transfer coefficient is calculated via a SINDA/FLUINT subroutine, EXTICYL, which calculates the forced convection heat transfer coefficient for a semi-infinite circular cylinder subject to a perpendicular external flow [Ref 3]. In user logic the total heat transfer coefficient is calculated as [Ref 3]:

$$\text{Eq. 11} \quad h_{\text{quench}} = h_{\text{film}} + h_{\text{conv}} \quad [\text{W/m}^2/\text{K}]$$

Any water vapor formed by the quench cooling water may be optionally added to the spray chamber model, Submodel “B”. Placing this additional vapor above the spray bar

in the spray chamber will create a greater load on the ejector pumps and cause the pressure in the spray chamber to rise.

Transient Control

For a transient model of the rocket exhaust duct flow the series of FASTIC steady state calls, as previously described (SINDA/FLUINT Modeling of Supersonic Flow), are called as desired by the user. A time increment for updating any rocket transient data is input through the SINDA/FLUINT Register Data Block. This transient data may include, but is not limited to, oxidizer to fuel weight ratio, and chamber pressure. The data may be input through the Array Data Block. The shocking and subsequent quenching of the rocket exhaust duct flow is respectively updated as well. However, the shocking and quenching of the duct flow may also be updated via a separate parameter during the transient analysis. The user may update this process as a function of change in spray chamber pressure via user logic. This incremental change of spray chamber pressure is input in the Register Data Block.

Model Details: Submodel “B”

Model Setup

The B2 spray chamber is modeled in FLUINT as a stratified vessel using a series of stacked “pancakes”, previously shown in Figure 5. The “pancakes” are modeled as FLUINT tanks with ifaces between them. The tanks have volume and therefore mass, and the ifaces are “massless” membranes that will expand or contract the tanks to which they are attached, as mass is either added or subtracted from said tanks. These ifaces maintain constant pressure between the tanks. Also between the tanks are set volume flow rate connectors (VFRSET). Logic was created to calculate the appropriate volume flows rate to pass between the “pancakes” so that the volumes of the “pancakes” would remain relatively equal, or more realistically, within a certain percentage of each other. These volume flows rate always flow “up” and never reverse, that is, flow always proceeds in the direction from the rocket exhaust duct plenum to the ejector pump plenum.

The shocked and quenched flow of the rocket exhaust duct enters the bottom of the spray chamber. In this analysis, this exhaust duct flow is comprised of steam and hydrogen. This inflow condition is modeled via a plenum with a set mass flow rate connector (MFRSET). These conditions are allowed to vary according to transient input data, as described in the previous section, **Model Details: Submodel “A”, Transient Control**. The outflow of the system is controlled by an ejector pumping system. This is modeled with a plenum and MFRSET connector. The ejector pumping capacity is input as mass flow rate versus pressure curves in the Register Data Block. These curves are used in the logic blocks to determine the appropriate amount of steam and hydrogen to remove from the system based on the spray chamber pressure. The ejector MFRSET connector utilizes

the species specific suction option to remove the appropriate amounts of steam and hydrogen based on the calculations using the ejector curves in the logic blocks.

The model contains lumps which are “dummy plenums” that don’t have any impact on the flow solution but are used for bookkeeping purposes. These lumps store the saturated pressure and the core temperature of the characteristic liquid droplet that occupies a respective tank at a given time. Every tank has associated with it a “dummy plenum” that represents a droplet with a unique inlet Sauter Mean Diameter (SMD). For example if there are five stratified “pancakes”, or tanks, and only one inlet SMD family of droplets, then there are five “dummy plenums”. If there are two families of droplets with different inlet SMDs then there are ten “dummy plenums”, or two “dummy plenums” for every tank. Figure 8 illustrates the B2 spray chamber modeled as a stratified vessel using five FLUINT tanks. There is only one inlet SMD family of droplets so there are only five “dummy plenums” which represent the properties of the characteristic droplet within the respective five tanks. Although referred to as plenums, these FLUINT lumps are input as tanks but are held in boundary states via FLUINT subroutine calls to HLDLMP. This procedure essentially makes the tanks behave as plenums. This is done once again for bookkeeping purposes. Before the calls to HLDLMP are made, the volumes of these tanks are updated to store the current liquid volume of the sum total of the droplets occupying it respective stratified tank.

The spray bar is modeled via a plenum with a set mass flow rate connector (MFRSET). Note that the location of the MFRSET connector will vary depending on how many tanks with which the user opts to stratify the spray chamber vessel. That is, the spray bar MFRSET will connect to the droplet “dummy plenum” whose respective stratified tank is at the approximate physical location of the spray bar. The spray bar plenum and its MFRSET connector, serve only to book keep the inlet water flow that enters the spray chamber.

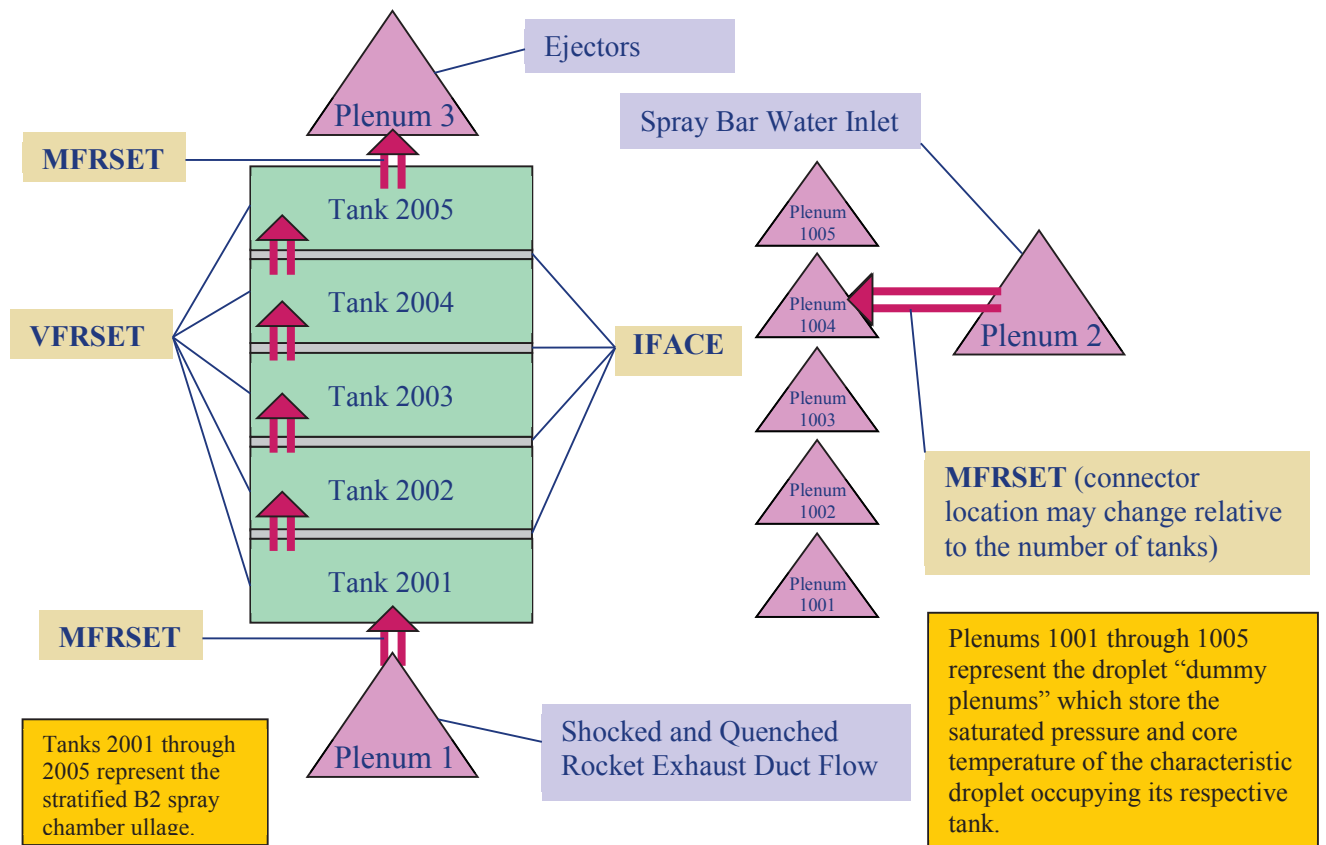


Figure 8: FLUENT Model Setup of Spray Chamber

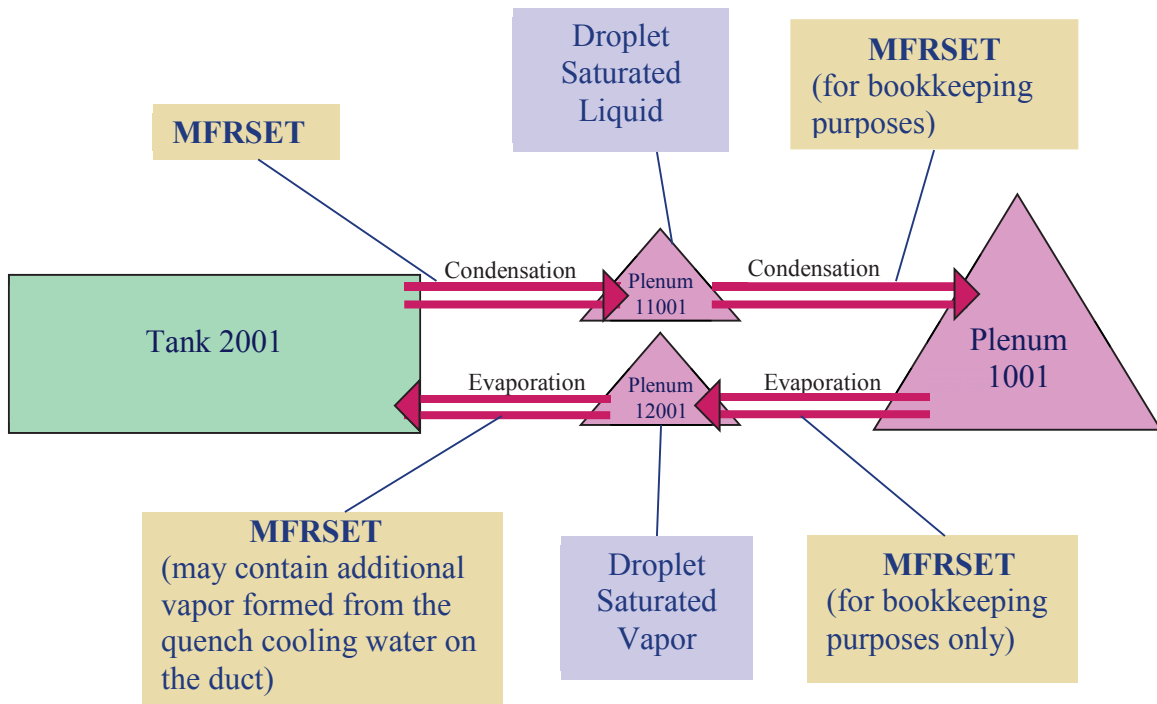


Figure 9: FLUINT Model Setup of Spray Chamber

Each tank and droplet “dummy plenum” has associated with it two plenums, refer to Figure 9, which illustrates this for only one tank and its respective droplet “dummy plenum”. These plenums are updated in user logic to be at the saturation pressure and temperature of the characteristic droplet that occupies that tank at a given time. One plenum represents the saturated liquid state, and the other plenum represents the saturated vapor state. Note that this saturation state may not necessarily be equivalent to the saturation state of the tank. The saturated liquid plenum has an MFRSET connector which removes the condensate mass flow rate from its respective tank, and an MFRSET connector which places the condensate mass flow rate into its corresponding droplet “dummy plenum”. The latter MFRSET is just for bookkeeping purposes and does not influence the solution. The saturated vapor plenum has an MFRSET connector which transfers the evaporative mass flow rate from the droplets to its respective tank, and an MFRSET connector which removes the evaporative mass flow rate from the droplets from its corresponding droplet “dummy plenum”. The latter MFRSET is just for bookkeeping purposes and does not influence the solution. The saturated vapor plenum’s MFRSET connector may optionally include vapor formed from the quench cooling water used on the outside wall of the rocket exhaust duct. The total vapor flow rate formed from the quench cooling water may be equally divided and distributed amongst all the tanks, or it may be distributed equally amongst the tanks that physically reside above the spray bars.

The shocked and quenched rocket exhaust duct flow rate that enters the spray chamber and passes through the stratified tanks never technically mixes with the spray bar inlet

water mass flow rate on the FLUINT level. That is, the spray bar water flow never occupies a FLUINT tank that contains the exhaust duct flow. The exhaust duct flow and the spray bar water flow follow counter flow paths that virtually run parallel to one another (see Figure 8). The water flow from the spray bar always flows “down” and is not modeled using MFRSET connectors because the water flow is not modeled as a continuum, but as droplets. The modeling of the droplet physics, momentum and heat transfer, is primarily accomplished through user logic. This is because it is desirable and more appropriate for the system being analyzed that the droplet mechanics be Lagrangian based. The FLUINT “pancake” is homogeneous and may be in thermal nonequilibrium with the droplets that reside in it at a given time. It is desired that a model be created that determines the condensing efficiency and not require this parameter as an input. Neither should the pressure distribution through the spray chamber ever be assumed but calculated in the model. Although the modeling of the droplet is Lagrangian based, tracking of individual droplets is not done. Rather, within each tank a time weighted average of droplet parameters is determined. These time weighted parameters represent the characteristic droplet that resides in a given tank at a given time. Also, for a given tank there is a characteristic droplet for each inlet SMD family of droplets.

Droplet Model: Momentum

The inflow water flow rate from the spray bar is modeled as an inflow of water droplets at a specified velocity. The droplets enter the spray chamber and interact with the FLUINT tank that physically resides at the approximate height of the spray bar. The exhaust duct flow through the VFRSET connectors does not include the drag force exerted upon it from the water droplets. However, the momentum of the water droplets does include the drag force exerted upon the water droplets from the exhaust duct flow. The relative velocity of a droplet that virtually resides in a FLUINT tank or “pancake” is defined by:

Eq. 12
$$V_{rel} = V_d + V_{\infty} \quad [m/s]$$

where V_{∞} is the velocity of the exhaust duct flow entering the VFRSET connector of the respective FLUINT tank (see Figure 10).

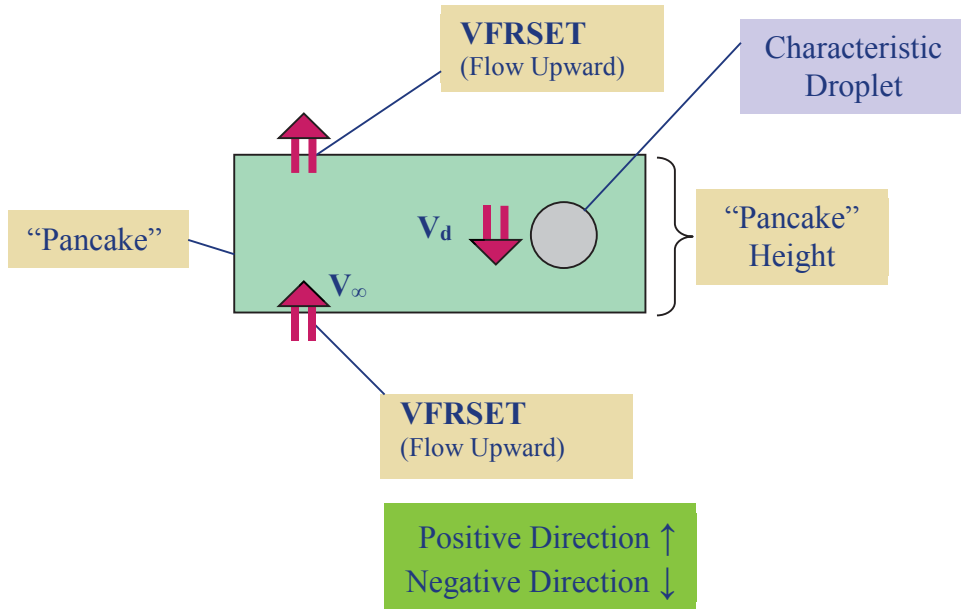


Figure 10: Characteristic Droplet in FLUINT Stratified Tank or "Pancake"

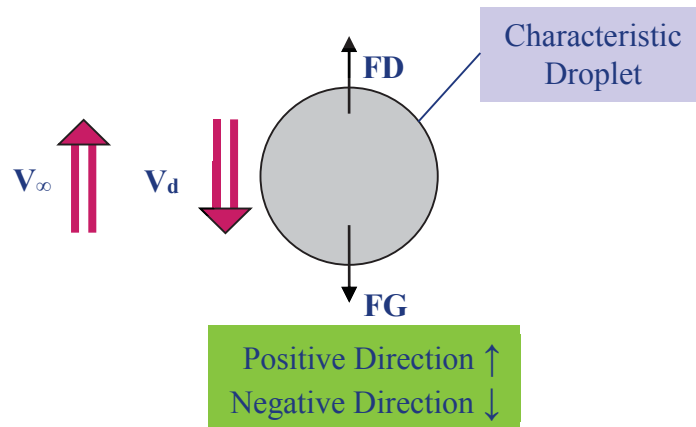


Figure 11: Forces Acting on a Droplet

The forces acting on the droplet are illustrated in Figure 11. The body force is defined by:

Eq. 13
$$FG = m_d g \quad [N]$$

or

Eq. 14
$$FG = \frac{4}{3} \pi r^3 (\rho_\infty - \rho_d) g \quad [N]$$

The drag force is determined via a drag coefficient defined by:

$$\text{Eq. 15} \quad C_D = \frac{-2.0 F_D}{\pi r_d^2 \rho_\infty V_{rel} |V_{rel}|}$$

The drag coefficient is determined via Schiller Naumanns relation [Ref 8] which is modified to have the correct limit for the inertial regime:

$$\text{Eq. 16} \quad C_D = \frac{24.0}{Re} \max\left(\left(1.0 + 0.15 Re^{0.687}\right), 0.44\right)$$

Figure 11 illustrate that the model always has the rocket exhaust duct flow through the VFRSET connectors go “up” or the positive direction, and the droplets flow “down” or the negative direction. From the FLUINT perspective, this is to avoid excessive flow reversals through the VFRSET connectors. User logic forces flow “upward” through a VFRSET connector if the volume of a given “pancake” is larger than the corresponding “pancake” above it, otherwise the flow rate through the VFRSET connector is zero. The droplets also do not experience flow reversal because of the complexity of book keeping them. If a characteristic droplet residing in a “pancake” at a given time experiences a net upward force the absolute velocity of the droplet will decrease until it reaches a value of zero. Once it reaches zero and continues to have a net upward force, the velocity continues to remain zero until there is a net downward force. During this time the characteristic droplet remains in its “pancake”. This in effect models “floating” droplets. Droplets from a “pancake” above a “pancake” with floating droplets are still allowed to enter the “pancake” where droplets are floating, given that the droplets in the above “pancake” are experiencing a net downward force. This will ultimately create an accumulation of droplets in the “pancake” still experiencing a net upward force with floating droplets thus causing that “pancake” to flood. The net force on the droplet is the sum of the body force and the drag force. The change in velocity of a droplet for a given time step is calculated via:

$$\text{Eq. 17} \quad F_G + F_D = m_d \frac{dV_d}{dt} \quad [N]$$

When a characteristic droplet travels the height of a “pancake” (see Figure 10) in which it currently resides at a given time, it will virtually pass to the “pancake” below. This means that all the droplets in the “pancake” move en mass to the “pancake” below. Because of this effect, there may be moments in time that a given “pancake” may be void of droplets. Another consequence of the droplets only being able to move “downward” is that droplets cannot virtually reside in any “pancake” above the spray bar.

The number of droplets entering the spray chamber through the spray bar is calculated knowing the Sauter Mean Diameters (SMD) of the inlet families of droplets. At a given time the total number of droplets that virtually reside in the “pancake” that is

approximately at the physical height of the spray bar can be determined. Each new set of droplets that enter this “pancake” are at the inlet spray bar conditions and have a uniform temperature. The droplets that already reside in this “pancake” may have a different velocity and a different temperature distribution. Since each individual droplet is not tracked, a characteristic droplet having a time averaged value of velocity and a time averaged temperature distribution must be determined. The characteristic droplet has a velocity determined via:

Eq. 18
$$V_d = \frac{V_{in_d} N_{drop_{in}} + (V_{old_d} + dV_d) N_{drop}}{N_{drop_{in}} + N_{drop}} \quad [m/s]$$

where dV_d is determined from Equation 17. The temperature distribution will be discussed in **Model Detail “Submodel B”, Droplet Model: Heat Transfer**.

Droplet Model: Heat Transfer

The heat transfer between the droplets in a “pancake” and the exhaust duct flow involves:

- sensible heat (conduction and convection) through the diffusion layer to the edge of the condensate layer over the droplet
- the latent heat released from the vapor of the exhaust duct flow condensing over the droplet
- sensible heat (conduction and convection) through the condensate layer over the droplet
- thermal conduction through the droplet (see Figure 4)

Figure 4 illustrates these heat transfer mechanisms.

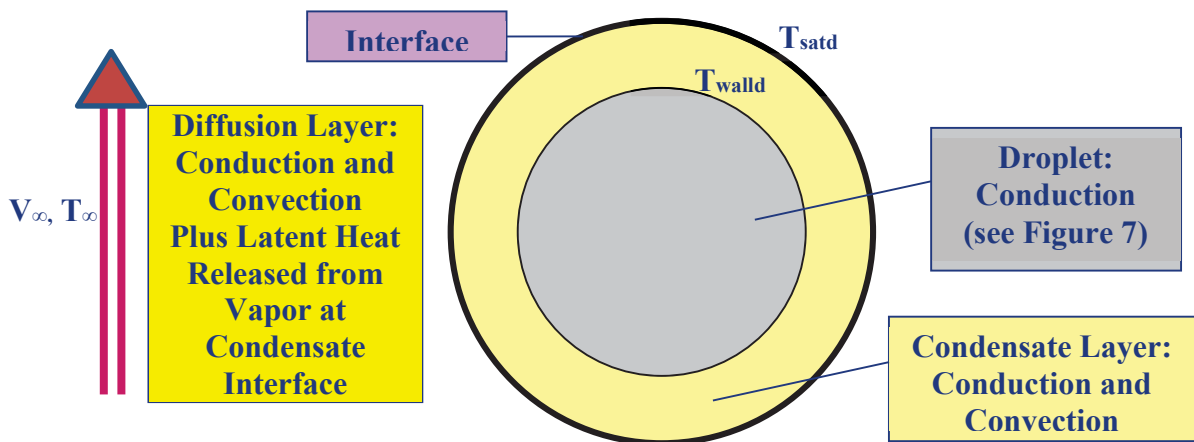


Figure 12: Heat Transfer Mechanisms between Exhaust Duct Flow and Droplet

The sensible heat (conduction transfer and convection transport) is modeled via Ranz Marshall [Ref 1]:

$$\text{Eq. 19} \quad \text{Nu} = 2.0 + 0.6 \text{Re}^{0.5} \text{Pr}^{0.33}$$

where Nu is the Nusselt Number. The heat transfer coefficient is determined by:

$$\text{Eq. 20} \quad \text{Nu} = \frac{h_{\text{conv}} D_d}{k}$$

The fluid properties are taken at a reference temperature using a simple 1/3 rule:

$$\text{Eq. 21} \quad T_{\text{ref}} = T_{\text{satd}} + \frac{(T_{\infty} - T_{\text{satd}})}{3} \quad [\text{K}]$$

The latent heat released from the water vapor in the exhaust duct flow condensing on the surface of a water droplet is determined by how much of this vapor is transported through the diffusion barrier of the noncondensable gas, hydrogen, building up next to the condensate layer. Reviewing Fick's Law, [Ref 9], for a binary system of hydrogen and water vapor in spherical coordinates the transfer of water vapor is:

$$\text{Eq. 22} \quad j_w = -\rho D_{wh} \frac{\delta x_w}{\delta r} \quad [\text{kg/s/m}^2]$$

and the transfer of hydrogen is:

$$\text{Eq. 23} \quad j_h = -\rho D_{wh} \frac{\delta x_h}{\delta r} \quad [\text{kg/s/m}^2]$$

The mass flux rates of water vapor and hydrogen are respectively:

$$\text{Eq. 24} \quad \dot{m}_w = \rho_w V_w \quad [\text{kg/s/m}^2]$$

$$\text{Eq. 25} \quad \dot{m}_h = \rho_h V_h \quad [\text{kg/s/m}^2]$$

The total average mass flux is:

$$\text{Eq. 26} \quad \rho V = \rho_w V_w + \rho_h V_h \quad [\text{kg/s/m}^2]$$

and the mass averaged mixture velocity is:

$$\text{Eq. 27} \quad V = x_w V_w + x_h V_h \quad [\text{m/s}]$$

The mass flux rates of water vapor and hydrogen consists of a diffusive part which is due to the relative velocity of the respective constituent to the mass averaged velocity of the mixture, and a convective part which is due to the "drift" of the respective constituent

with the mass averaged velocity of the mixture. Thus the absolute mass flux rates of water vapor and hydrogen respectively become:

$$\text{Eq. 28} \quad \dot{m}_w = -\rho D_{wh} \frac{\delta x_w}{\delta r} + x_w (\dot{m}_h + \dot{m}_w) \quad [\text{kg/s/m}^2]$$

$$\text{Eq. 29} \quad \dot{m}_h = -\rho D_{wh} \frac{\delta x_h}{\delta r} + x_h (\dot{m}_h + \dot{m}_w) \quad [\text{kg/s/m}^2]$$

The above equations are subject to the condition:

$$\text{Eq. 30} \quad x_w + x_h = 1$$

Under steady state conditions the mass flow rate of water vapor in the radial direction does not change:

$$\text{Eq. 31} \quad \frac{\delta(\dot{m}_w 4\pi r^2)}{\delta r} = \frac{\delta(\dot{m}_w)}{\delta r} = 0 \quad [\text{kg/s/m}^2]$$

The noncondensable gas, hydrogen, is taken to be insoluble in liquid water (i.e., at the surface of the water droplet). Under steady state conditions this translates to the mass flux rate of hydrogen being zero:

$$\text{Eq. 32} \quad \dot{m}_h = 0 \quad [\text{kg/s/m}^2]$$

If Equation 32 is imposed upon Equation 29 the result is:

$$\text{Eq. 33} \quad \rho D_{wh} \frac{\delta x_h}{\delta r} = x_h \dot{m}_w \quad [\text{kg/s/m}^2]$$

In other words, during condensation, a driving diffusive force of hydrogen away from the droplet surface must exactly counterbalance the convective flow of the hydrogen toward the surface [Ref 10]. During condensation the noncondensable hydrogen gas accumulates at the surface of the water droplet. The partial pressure of the hydrogen at the surface of the droplet actually becomes larger than the partial pressure of the hydrogen in the bulk or exhaust duct flow. This build up of noncondensable gas has a significant effect on the heat transfer because the mass transfer of the water vapor is decreased because of the diffusion barrier. Also since the total pressure remains constant, at the droplet surface where the hydrogen partial pressure has increased the partial pressure of the water vapor falls below the saturation pressure of the water vapor in the bulk or exhaust duct flow. In turn this reduces the saturation temperature, T_{satd} , at which condensation occurs.

Applying Equation 32 to Equation 28 results in:

$$\text{Eq. 34} \quad \dot{m}_w = \frac{-\rho D_{wh} \frac{\delta x_w}{\delta r}}{1 - x_w} \quad [\text{kg/s/m}^2]$$

Applying Equation 31 to Applying Equation 34 results in:

$$\text{Eq. 35} \quad \dot{m}_w = \frac{-4\pi r^2 \rho D_{wh} \frac{\delta x_w}{\delta r}}{1 - x_w} \quad [\text{kg/s}]$$

or

$$\text{Eq. 36} \quad \frac{\dot{m}_w \partial r}{r^2} = \frac{-4\pi \rho D_{wh} \partial x_w}{1 - x_w} \quad [\text{kg/s/m}]$$

Integrating from the droplet surface to infinity, i.e. the exhaust duct flow, we obtain

$$\text{Eq. 37} \quad -\frac{\dot{m}_w}{r} \Big|_{r_1}^{r_\infty} = 4\pi \rho D_{wh} \ln(1 - x_w) \Big|_{r_1}^{r_\infty} \quad [\text{kg/s/m}]$$

or

$$\text{Eq. 38} \quad \dot{m}_w = 4\pi r_s \rho D_{wh} \ln\left(\frac{1 - x_{w\infty}}{1 - x_{wi}}\right) \quad [\text{kg/s}]$$

The mass flux rate then becomes:

$$\text{Eq. 39} \quad \dot{m}_w = \frac{\rho D_{wh}}{r_s} \ln\left(\frac{1 - x_{w\infty}}{1 - x_{wi}}\right) \quad [\text{kg/s/m}^2]$$

A negative value for the mass flow rate or the mass flux rate corresponds to “suction” or condensation on the droplet surface. The density in Equation 39 is evaluated at the reference temperature defined in Equation 21. If a Lewis number of one is assumed, i.e. the ratio of thermal diffusivity to mass diffusivity is equal to one, Equation 39 may be replaced by:

$$\text{Eq. 40} \quad \dot{m}_w = \frac{k}{C_p r_s} \ln\left(\frac{1 - x_{w\infty}}{1 - x_{wi}}\right) \quad [\text{kg/s/m}^2]$$

The heat transfer rate from the “bulk” or rocket exhaust duct flow to the droplet interface is:

$$\text{Eq. 41} \quad Q_{\infty} = A s_s \left(\frac{k}{C_p r_s} \ln \left(\frac{1 - x_{w\infty}}{1 - x_{wi}} \right) h'_{fg} + h_{\text{conv}} (T_{\infty} - T_{\text{satd}}) \right) \quad [\text{W}]$$

In a quasi-steady process this heat rate must equal the heat rate through the condensate layer. In the condensate layer the rate of heat transfer may be defined as:

$$\text{Eq. 42} \quad Q_{\text{cond}} = A s_s h_{\text{cond}} (T_{\text{satd}} - T_{\text{walld}}) \quad [\text{W}]$$

In order to solve for T_{satd} , Equation 41 and Equation 42 must be iteratively solved. Basically one would guess an initial T_{satd} , usually a value between $T_{\text{sat}\infty}$ and T_{walld} . Once T_{satd} is known the mass fraction x_{wi} may be determined.

The condensation heat transfer coefficient is that for condensation on a rigid sphere [Ref 1] with the following assumptions:

- the temperature distribution in the condensate film is linear
- axial conduction is neglected
- shear forces at the interface are neglected

Chung and Ayyaswamy, [Ref 1], make use of a correlation that includes inertial effects, (usually only film conduction is considered):

$$\text{Eq. 43} \quad h_{\text{cond}} = 1.098 \left(\frac{k_{\ell}^3 g (\rho_{\ell} - \rho_v) h'_{fg}}{\mu_{\ell} D_d (T_{\text{satd}} - T_{\text{walld}})} \right)^{0.25} \quad [\text{W/m}^2/\text{K}]$$

Droplet Model: Heat Transfer Applied in SINDA/FLUINT

Within the SINDA/FLUINT model an iterative technique similar to the one described in the previous section to calculate T_{satd} is accomplished using a SINDA/FLUINT subroutine, HTUDIF, [Ref 4]. This subroutine uses the general purpose Chilton-Coulburn analogy:

$$\text{Eq. 44} \quad \frac{h_{\text{conv}} (\rho_{w\infty} - \rho_{wi})}{m_w} = \left[\frac{P_{\text{tot}}}{P_{h\infty}} \rho_{h\infty} \frac{\ln \left(\frac{\rho_{hi}}{\rho_{h\infty}} \right)}{(\rho_{hi} - \rho_{h\infty})} \right]^{-1} \left[\rho_{\infty} C_{p\infty} \left(\frac{k_{\infty}}{D_{wh}} \right)^2 \right]^{1/3} \quad [\text{J/m}^3/\text{K}]$$

The interfacial temperature, T_{satd} , is iteratively solved for using the following energy balance:

$$\text{Eq. 45} \quad h_{\text{cond}}(T_{\text{satd}} - T_{\text{walld}}) = \dot{m}_w h'_{\text{fg}} + h_{\text{conv_HTUDIF}}(T_{\infty} - T_{\text{satd}}) \quad [\text{W/m}^2]$$

$$= h_{\text{eff}}(T_{\text{sat}\infty} - T_{\text{walld}})$$

For a given “pancake” or stratified tank the subroutine requires the following input:

- Temperature of the mixture in the “pancake”
- Absolute pressure of mixture in the “pancake”
- Wall temperature (i.e., T_{walld})
- Mixture heat transfer coefficient (i.e., $h_{\text{conv_HTUDIF}}$)
- Condensation heat transfer coefficient (i.e., h_{cond})

The subroutine returns h_{eff} , the effective heat transfer coefficient between the vapor saturation temperature in the “pancake” and the droplet wall temperature. Equation 45 is then used to calculate T_{satd} . HTUDIF is called within the SINDA/FLUINT logic block, FLOGIC 0. It is important to note that Submodel “B” runs as a full transient. The implementation of the aforementioned logic implies a quasi-steady solution of the droplet interfacial temperature (droplet saturation temperature) at a given time step.

The amount of condensate formed in a “pancake” at a given time is determined from Equation 43:

$$\text{Eq. 46} \quad \dot{m}_{\text{cond}} = \frac{A_s h_{\text{cond}} (T_{\text{satd}} - T_{\text{walld}})}{h'_{\text{fg}}} N_{\text{drop}} \quad [\text{kg/s}]$$

This mass flow rate is removed from its respective “pancake” via an MFRSET connector with a species specific option to remove only water vapor. This MFRSET is illustrated in Figure 9 as the condensation MFRSET between Tank 2001 and Plenum 11001. However the MFRSET is removing water vapor at the absolute temperature of Tank 2001 and not at the actual interfacial temperature (droplet saturation temperature) T_{satd} . The

consequence of this is that the correct mass rate is being removed from the tank but not the correct energy rate and therefore a correction must be made to the energy input to the tank. The energy that is being removed from said tank via the MFRSET connector is:

$$\text{Eq. 47} \quad Q_{\infty} = \dot{m}_{\text{cond}} H_{w\infty} N_{\text{drop}} \quad [\text{W}]$$

It should be:

$$\text{Eq. 48} \quad Q_{\infty} = \dot{m}_{\text{cond}} H_{\text{satv}} N_{\text{drop}} \quad [\text{W}]$$

A heat rate must thus be applied to the tank. This applied heat rate should be:

$$\text{Eq. 49} \quad \dot{Q}_L = (\dot{m}_{\text{cond}} H_{w\infty} - \dot{m}_{\text{cond}} H_{\text{satv}}) N_{\text{drop}} \quad [\text{W}]$$

Basically Equation 49 “replaces” the energy lost in the tank through the MFRSET connector and removes the correct energy from the tank.

Finally the convective heat rate leaving the tank must be included. The correct heat rate on a “pancake” or stratified tank is:

$$\text{Eq. 50} \quad \dot{Q}_L = [\dot{m}_{\text{cond}} H_{w\infty} - \dot{m}_{\text{cond}} H_{\text{satv}} - A_{S_s} h_{\text{conv}} (T_{\infty} - T_{\text{satd}})] N_{\text{drop}} \quad [\text{W}]$$

It should be noted that the amount of condensate formed is equally distributed among the number of droplets. The net increase in droplet diameter is negligible but book kept nonetheless.

An issue that arises in the model occurs when the solution reaches steady state conditions. Implementation of the aforementioned logic is done at the beginning of a time step, and does not change as a solution is iterated upon within the internal solver of SINDA/FLUINT. The condensation rate that occurs within a “pancake” is constant and based on all the droplets that reside in that “pancake” as the solver finds a solution for that time step. The heat and mass transfer rates do not reflect the change in the partial pressure of the water vapor of the “pancake” that occurs as the solver attempts to find a solution for the given heat and mass transfer rates assigned at the beginning of the time step. Thus the partial pressure of the water vapor in the “pancake” may drop below the droplet saturation temperature because of the inability to correct for the heat and mass transfer rates as the partial pressure of the water vapor changes. The overestimation of the heat and mass transfer rates must be accomplished on the next time step, at which condensation will not occur but *evaporation* will. The mass flow rate of evaporation is similar to that of Equation 38:

$$\text{Eq. 51} \quad \dot{m}_{\text{evap}} = A_{S_s} CF \left(\frac{k}{C_p r_s} \ln \left(\frac{1 - P_{w\infty}}{1 - P_{wi}} \right) \right) \quad [\text{kg/s}]$$

However, the mass fractions are replaced by partial pressures and a correction factor was added:

$$\text{Eq. 52} \quad CF = 2.0 + 0.6 \text{Re}^{0.5} \text{Pr}^{0.33}$$

This correction factor accounts for the enhancement of evaporation due to convection [Ref 11].

Instead of flow leaving the “pancake”, water vapor flows into the “pancake” via an MFRSET connector. This MFRSET is illustrated in Figure 9 as the evaporation MFRSET between Tank 2001 and Plenum 12001. Plenum 12001 is updated every time step to be the saturated vapor state of the characteristic droplet residing in Tank 2001.

The heat rate on the “pancake” now becomes:

$$\text{Eq. 53} \quad QL = [-As_s h_{\text{conv}}(T_\infty - T_{\text{satd}})]N_{\text{drop}} \quad [\text{W}]$$

Also since condensation occurs at T_{satd} which is lower than the saturation temperature of the water vapor in the FLUINT “pancake”, a very small amount of liquid may form when over-condensation occurs. If the quality becomes less than one, and T_{sat} is less than T_{satd} the heat rate on the “pancake”, is modified to be:

$$\text{Eq. 54} \quad QL = [-As_s h_{\text{conv}}(T_\infty - T_{\text{satd}}) + As_s h_{\text{film}_d}(T_{\text{satd}} - T_{\text{sat}})(1 - XL)]N_{\text{drop}} \quad [\text{W}]$$

where

$$\text{Eq. 55} \quad h_{\text{film}_d} = 0.62 \left(\frac{k_v^3 g \rho_v (\rho_l - \rho_v) h'_{\text{fg}}}{\mu_v D_d (T_{\text{satd}} - T_{\text{sat}})} \right)^{0.25} \quad [\text{W/m}^2/\text{K}]$$

The second term in Equation 54 accounts for the vaporization of any liquid mass fraction that may occur in the “pancake”.

As the solution approaches a steady state the spray chamber pressure, as will be seen in the **Results** section, will tend to oscillate about a small pressure dead band. These oscillations can be minimized by reducing the FLUINT control variable, DTSIZE, thereby reducing the amount a lump property can change in a time step. Another way to minimize the oscillations is to use one of SINDA/FLUINT’s more robust matrix solvers, i.e. setting MATMET = 12. Finally one can increase the number of “pancakes” or stratified tanks. The aforementioned procedures may create longer run times and smaller time steps.

Model Details: Submodel “C”

Model Setup

It is important to accommodate the physics of thermal conduction through the droplet in the SINDA/FLUINT model of the B2 facility. It is hypothesized that given the droplet sizes (on the order of 1500 microns and greater), droplet velocities (on the order of 37 m/s), and size of the spray chamber, that the water droplets may not be fully utilized. Therefore SINDA “solid conduction” droplets that correspond to each of the time averaged characteristic droplets are modeled. A SINDA droplet that models the thermal conduction through the droplet corresponds to, in time and space, the characteristic

droplet of a FLUINT “pancake” discussed in the section, **Model Details: Submodel “B”, Momentum**.

The number of thermal droplets created in the model equals the number of “pancakes” in the FLUINT model multiplied by the number droplet families (initial droplet sizes with varying SMDs). The degree of nodalization of the thermal droplet is determined by the user. For the current analysis the thermal droplets have ten nodes. The conductors between the nodes are defined by Equation 1. All conductors and capacitances are updated as a function of time and temperature in user logic.

These thermal droplets track the characteristic droplets created in the user logic blocks of the FLUINT portion of the model. That is, the time averaged properties of the droplet are overlaid onto the thermal droplet on the beginning of a time step in the thermal model. For the thermal model, the property of interest is the temperature distribution through the droplet. At the end of the time step the thermal model has solved for a new temperature distribution through a given droplet. This is the new temperature distribution for the characteristic droplet that is sent to the FLUINT user logic blocks. In the FLUINT logic blocks the droplet momentum equations are executed to determine whether droplets have left a given “pancake” and entered the “pancake” below. It is after this sequence of logic that a time average of droplet properties occurs. Equation 18 determines the new time averaged velocity of a characteristic droplet. However, whereas there is only one velocity per droplet, there is an entire temperature distribution per droplet. In the current analysis there are ten temperatures per droplet, corresponding to the ten nodes within the droplet. Therefore a time averaged temperature of each thermal node must be calculated. If $T^n_{in_d}$ is the temperature of the n^{th} node of a thermal droplet entering a “pancake” and $T^n_{old_d}$ is the temperature of the n^{th} node of a thermal droplet already in that “pancake”, then the new time averaged temperature of the characteristic droplet is:

$$\text{Eq. 56} \quad T^n_d = \frac{T^n_{in_d} N_{drop_{in}} + (T^n_{old_d}) N_{drop}}{N_{drop_{in}} + N_{drop}} \quad [K]$$

The SINDA VARIABLES 1 logic block of the droplet thermal model does a check to determine if there are any droplets residing in a given “pancake” at the current time step. As mentioned previously in the section, **Model Details: Submodel “B”, Momentum**, there may be moments in time that there are no droplets in a “pancake”. If there are no droplets in a “pancake”, the thermal nodes representing the droplet are placed in a boundary state. If droplets are present, the thermal nodes of the droplet are set to the distribution determined in the FLUINT FLOGIC 0 block determined by Equation 56. Also a heat rate from the condensation that occurs is applied to the outer most node of the droplet:

$$\text{Eq. 57} \quad Q_d = \dot{m}_{cond} h'_{fg} \quad [W]$$

It is not advisable to actually create a node that represents the condensate layer that forms around the droplet. This is because the layer is so thin and the thermal conductor so large

relative to the thermal conductors in the rest of the droplet that time step precipitously drops.

If evaporation occurs, the heat rate on the droplet, becomes:

$$\text{Eq. 58} \quad Q_d = [A_s h_{\text{conv}} (T_\infty - T_{\text{satd}}) - \dot{m}_{\text{evap}} h'_{\text{fg}}] \quad [\text{W}]$$

If T_{sat} is less than T_{satd} :

$$\text{Eq. 59} \quad Q_d = [A_s h_{\text{conv}} (T_\infty - T_{\text{satd}}) - A_s h_{\text{film}_d} (T_{\text{satd}} - T_{\text{sat}})(1 - XL) - \dot{m}_{\text{evap}} h'_{\text{fg}}] \quad [\text{W}]$$

Results

Model results were compared to four Delta III upper stage hot fire tests that were run in the B2 facility. Figure 13 illustrates a summary table of the four hot fire runs. In all the cases presented below the droplets leaving the spray bar were 1500 microns in size and had an initial velocity 37 ft/sec.

	HOT FIRE 3	HOT FIRE 6	HOT FIRE 8	HOT FIRE 10
CONDENSING SPRAY CONDITIONS				
INLET CONDENSING SPRAY TEMPERATURE (DEG F)*	50.6	51.5	55.99	64.2
INLET CONDENSING SPRAY FLOW RATE (KG/SEC)	13878	13878	13878	13878
WATER LEVEL (FT)	67.8	73.8	73.6	64.5
ULLAGE LENGTH (FT)	45.65	45.65	45.65	45.65
ROCKET CONDITIONS				
ROCKET EXIT AREA (IN ²)	1500	1500	1500	1500
ROCKET AREA RATIO	77	77	77	77
ROCKET O/F RATIO	6	6	6	6
ROCKET COMBUSTION PRESSURE (PSI)	640	640	640	640

* For spray bar temperature rise due to engine heat exhaust or ejector heat output this was only an initial condition.

Figure 13: Summary Table of Delta III Upper Stage Hot Fire Tests

Figure 14 through Figure 17 illustrate individual test data cases compared to the respective SINDA/FLUINT model results. The models were first run with the following assumptions (i.e., **Model ‘Hot Fire Case #’**):

- Steam formed from quench cooling along the rocket exhaust duct outside walls was neglected
- Spray bar temperature rise from the heat of the engine exhaust.

New model results were generated that included these two effects, (refer to output: **Model ‘Hot Fire Case #’ New**).

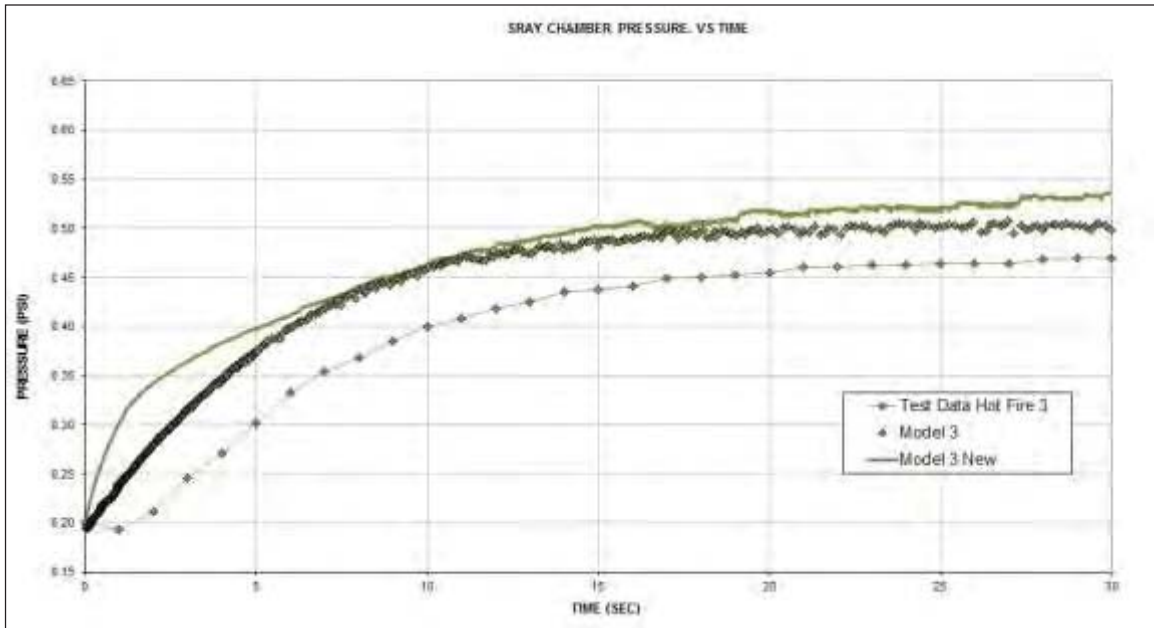


Figure 14: Spray Chamber Pressure: Hotfire Test 3 and SINDA/FLUINT Model Results

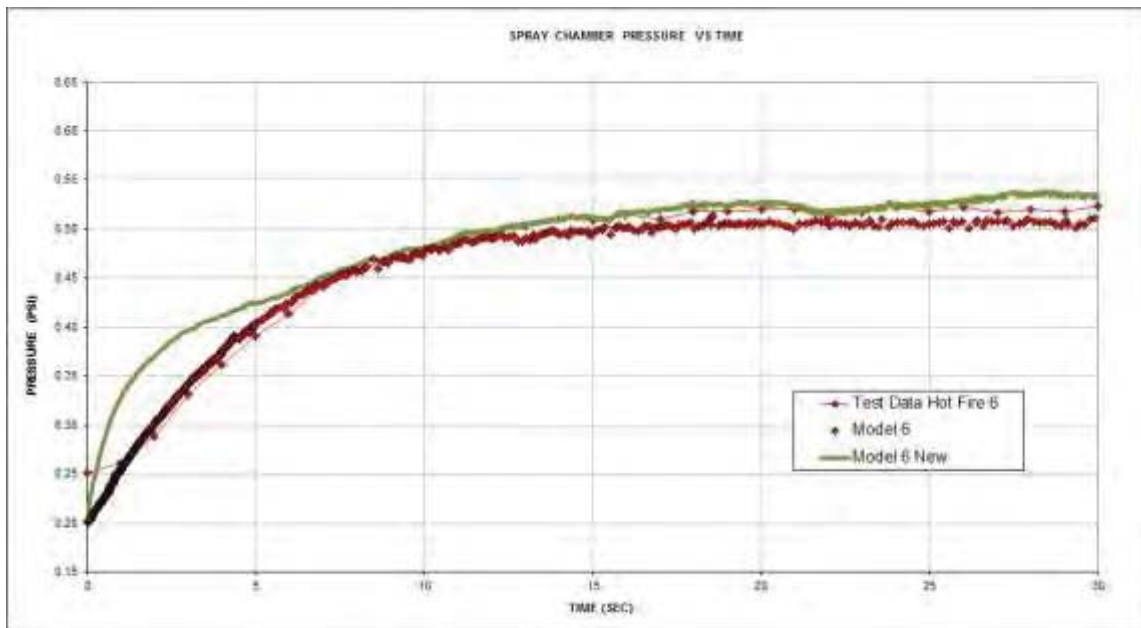


Figure 15: Spray Chamber Pressure: Hotfire Test 6 and SINDA/FLUINT Model Results

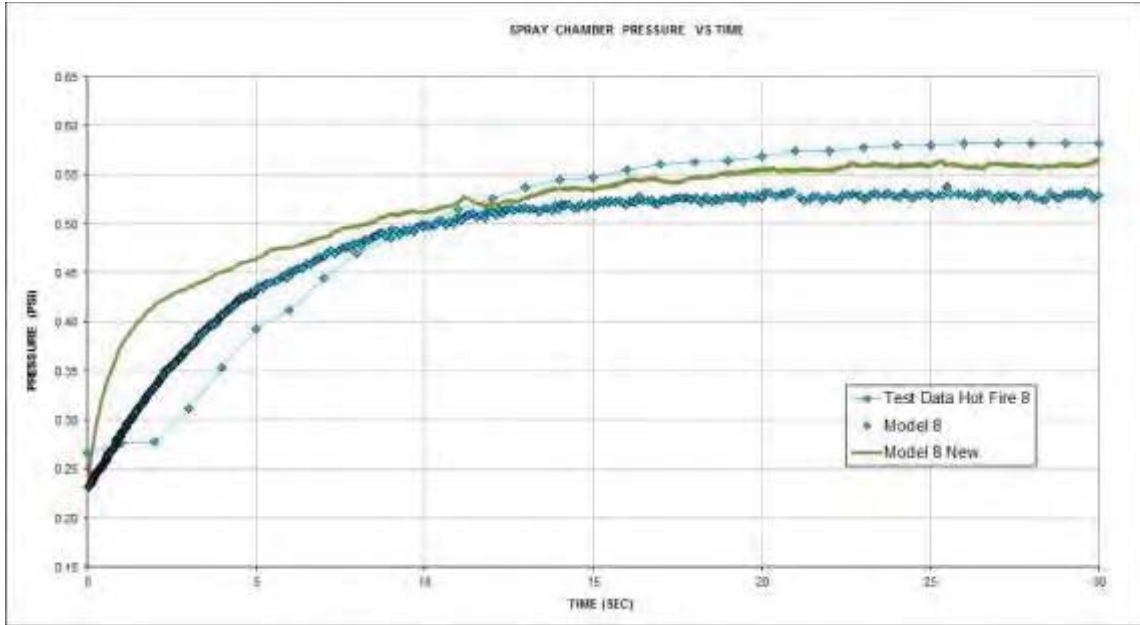


Figure 16: Spray Chamber Pressure: Hotfire Test 8 and SINDA/FLUINT Model Results

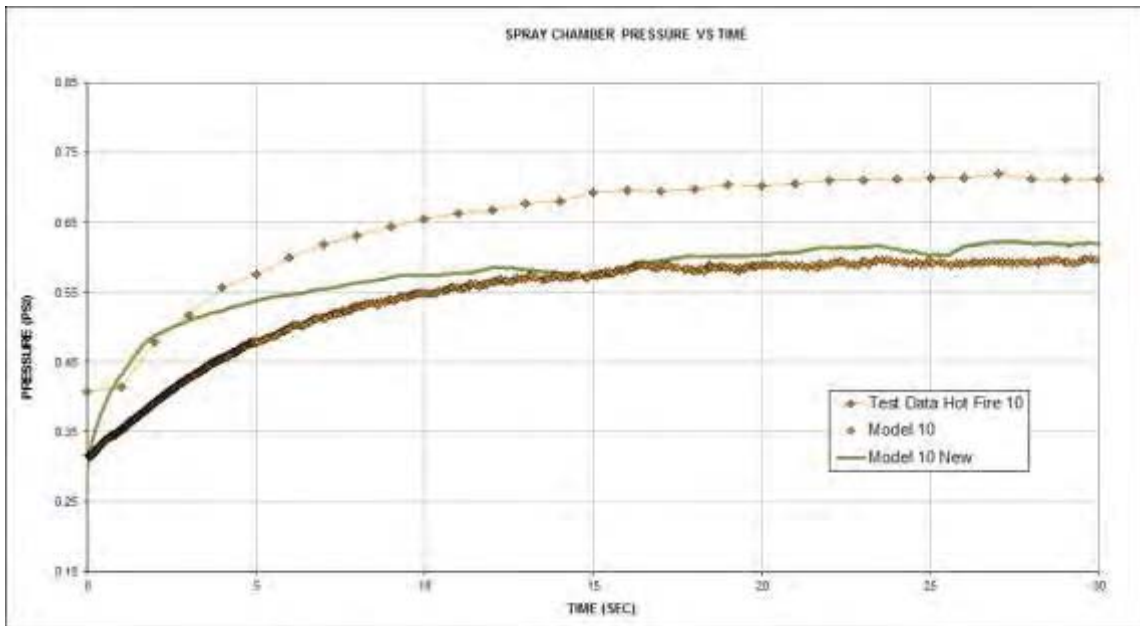


Figure 17: Spray Chamber Pressure: Hotfire Test 10 and SINDA/FLUINT Model Results

To examine effects of a candidate test article larger than the previously conducted engine tests at B-2, the SINDA/FLUINT Model was run using a two point engine test sequence lasting for 700 seconds. Figure 18 summarizes the significant input conditions used for this simulation. This model assumed the droplets leaving the spray bar were 1500 microns in size and had an initial velocity 37 ft/sec. The assumption that the spray bar water temperature rose due to the effect of engine exhaust heat was included in this analysis. Also vapor quench from cooling of the rocket exhaust duct was included. Figure 19 and Figure 20 provide the model outputs for spray chamber pressure and temperature. The useful result shown in these graphs are that the exhaust system , as

modeled, can support a 700 second duration engine firing where the initial engine thrust is higher followed by a lower thrust setpoint. The model can be useful in predicting exhaust system performance for various hydrogen-oxygen engine combinations and testing durations. Future engine testing at B-2 will provide opportunities to evaluate and refine the model.

	Candidate Test Article, First 400 sec.	Candidate Test Article, Last 300 sec.
CONDENSING SPRAY CONDITIONS		
INLET CONDENSING SPRAY TEMPERATURE (DEG F)*	40	40
INLET CONDENSING SPRAY FLOW RATE (KG/SEC)	13878	13878
WATER LEVEL (FT)	70	70
ULLAGE LENGTH (FT)	49.25	49.25
ROCKET CONDITIONS		
ROCKET EXIT AREA (IN ²)	5627	5627
ROCKET AREA RATIO	243	243
ROCKET O/F RATIO	5.797	5.826
ROCKET COMBUSTION PRESSURE (PSI)	882	637

* For spray bar temperature rise due to engine heat exhaust or ejector heat output this was only an initial condition.

Figure 18: Summary Table of Candidate Test Article Input

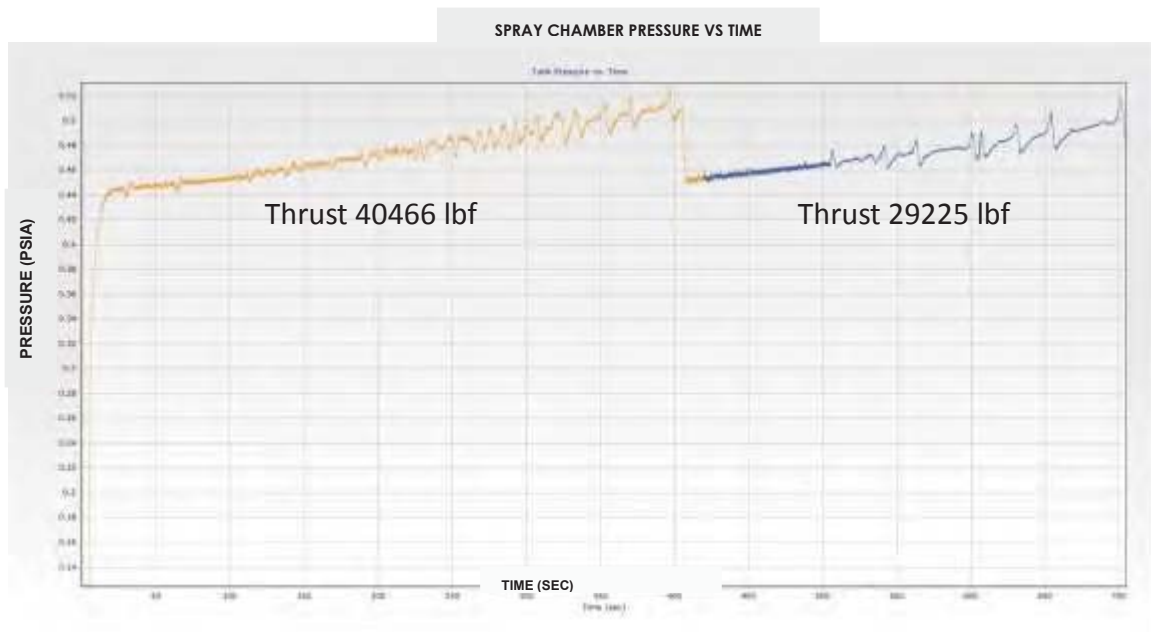


Figure 19: Spray Chamber Pressure for Candidate Test Article SINDA/FLUINT Model Results

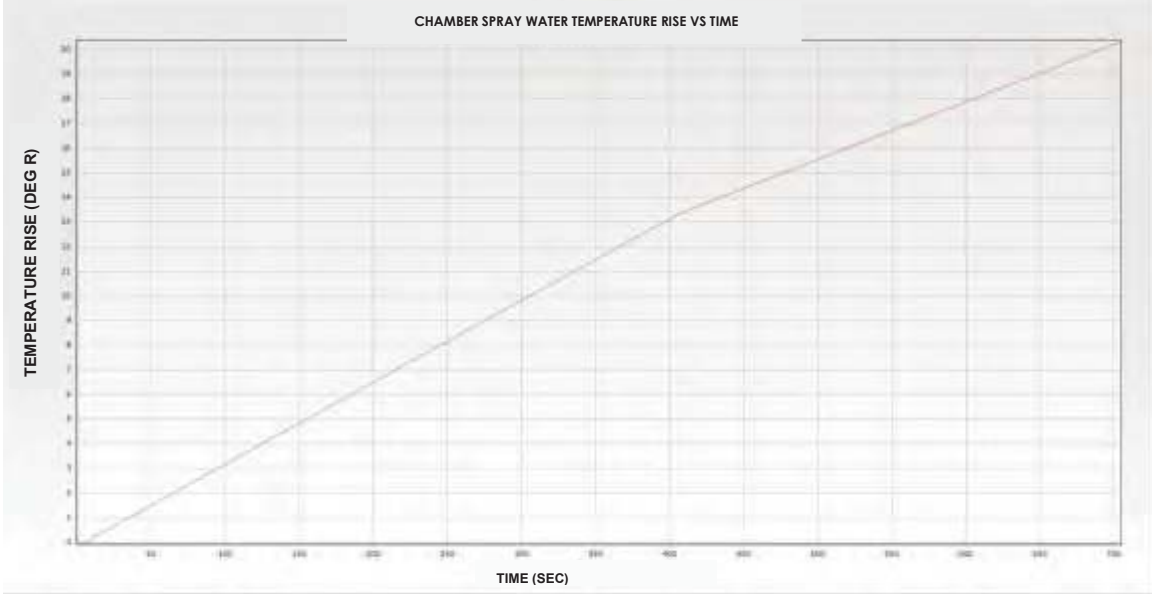


Figure 20: Chamber Spray Water Temperature Rise for Candidate Test Article SINDA/FLUINT Model Results

Acknowledgements:

Kevin Dickens

Appendix A: CEA and SINDA/FLUINT Enthalpy and Entropy Reference States

The relationship between the H₂O enthalpies of REFPROP and CEA is as follows:

$$\text{Eq. A.1} \quad H_{\text{CEA}} = H_f + (H_{\text{REFPROP}} - H_{\text{REFPROP_satvap_298}}) \quad [\text{KJ/kg}]$$

where H_f is the enthalpy of formation of H₂O vapor at 298.15 K and 0.1 MPA. It should be noted that the default setting for the reference state was set in REFPROP. Example A.1 illustrates the use of Eq. 1 with the aid of Tables A.1 through A.3.

Example A.1: Steam at 629.0 K and 0.1 MPA

$$H_{\text{CEA}} = -13423.647 + (3187.8 - 2546.5) = -12782.3 \quad [\text{KJ/kg}]$$

Inspecting Table A.2, CEA's output enthalpy of -12781.3 KJ/kg compares well to Example A.1.

The relationship between the H₂O entropies of REFPROP and CEA is as follows:

$$\text{Eq. A.2} \quad S_{\text{CEA}} = S_f + (S_{\text{REFPROP}} - S_{\text{REFPROP_satliq_298}}) \quad [\text{KJ/kg/K}]$$

where S_f is the absolute entropy of H₂O liquid at 298.15 K and 0.1 MPA. Example A.2 illustrates the use of Eq. 2 with the aid of Tables A.1 through A.3.

Example A.2: Steam at 629.0 K and 0.1 MPA

$$S_{\text{CEA}} = 3.882 + (8.4057 - 0.36722) = 11.923 \quad [\text{KJ/kg/K}]$$

Inspecting Table A.2, CEA's output entropy of 11.922 KJ/kg/K compares well to Example A.2.

Table A.1: REFPROP Output of H₂O Properties [Ref 5]

TEMPERATURE K (SATURATED)	PRESSURE MPA	LIQUID DENSITY kg/m ³	VAPOR DENSITY kg/m ³	LIQUID ENTHALPY KJ/kg K	VAPOR ENTHALPY KJ/kg	LIQUID ENTROPY KJ/kg/K	VAPOR ENTROPY KJ/kg/K
298.15	0.0031699	997.0	0.023075	104.83	2546.5	0.36722	8.5566

TEMPERATURE K	PRESSURE MPA	DENSITY kg/m ³	ENTHALPY KJ/kg	ENTROPY KJ/kg/K
629.00	0.1	0.34506	3187.8	8.4057

Table A.2: CEA Output of H₂O Properties [Ref 6]

THERMODYNAMIC EQUILIBRIUM PROPERTIES AT ASSIGNED
TEMPERATURE AND PRESSURE

CHEMICAL FORMULA	WT FRACTION	ENERGY	STATE	TEMP
FUEL H 2.00000 O 1.00000		KJ/KG-MOL	DEG K	
O/F = 0.0000 PERCENT FUEL = 100.0000		1.000000	0.000	G 629.00
	EQUIVALENCE RATIO = 1.0000		PHI = 0.0000	

THERMODYNAMIC PROPERTIES

P, MPA	0.10002
T, DEG K	629.00
RHO, KG/CU M	3.4455-1
H, KJ/KG	-12781.3
U, KJ/KG	-13071.6
G, KJ/KG	-20280.2
S, KJ/(KG)(K)	11.9220

M, MOL WT	18.015
(DLV/DLP)T	-1.00000
(DLV/DLT)P	1.0000
CP, KJ/(KG)(K)	2.0348
GAMMA (S)	1.2934
SON VEL,M/SEC	612.7

TRANSPORT PROPERTIES (GASES ONLY)
CONDUCTIVITY IN UNITS OF MILLIWATTS/(CM)(K)

VISC,MILLIPOISE 0.22572

WITH EQUILIBRIUM REACTIONS

CP, KJ/(KG)(K)	2.0348
CONDUCTIVITY	0.4969
PRANDTL NUMBER	0.9243

WITH FROZEN REACTIONS

CP, KJ/(KG)(K)	2.0348
CONDUCTIVITY	0.4969
PRANDTL NUMBER	0.9243

MOLE FRACTIONS

H2O	1.00000
-----	---------

Table A.3: CEA Output of H₂O Liquid Properties [Ref 6]

THERMODYNAMIC EQUILIBRIUM PROPERTIES AT ASSIGNED
TEMPERATURE AND PRESSURE

CHEMICAL FORMULA	WT FRACTION	ENERGY	STATE	TEMP
	KJ/KG-MOL	DEG K		
FUEL H 2.00000 O 1.00000	1.000000	0.000	L	298.15
O/F = 0.0000 PERCENT FUEL = 100.0000	EQUIVALENCE RATIO = 1.0000			
		PHI = 0.0000		
 THERMODYNAMIC PROPERTIES				
P, MPA	0.10002			
T, DEG K	298.15			
RHO, KG/CU M	1.0799 6			
H, KJ/KG	-15866.2			
U, KJ/KG	-15866.2			
G, KJ/KG	-17024.1			
S, KJ/(KG)(K)	3.8835			
 M, MOL WT *****				
(DLV/DLP)T	-0.19929			
(DLV/DLT)P	1.1114			
CP, KJ/(KG)(K)	4.1821			
GAMMA (S)	5.0179			
SON VEL,M/SEC	0.7			
 MOLE FRACTIONS				
H2O(L)	1.00000			

The relationship between the H₂ enthalpies of REFPROP and CEA, using the default reference setting, is not as straight forward. The CEA enthalpy is defined by:

$$\text{Eq. A.3} \quad H_{\text{CEA}} = (H_{\text{REFPROP}} - H_{\text{ASSIGNED}}) \quad [\text{KJ/kg}]$$

noting that the heat of formation is zero. The assigned enthalpy, H_{ASSIGNED}, for liquid or vapor H₂ is 9.012 KJ/mole or 4470 KJ/kg. The assigned enthalpy for superheated H₂ is the enthalpy of H₂ at 298.15 K and 0.1 MPA. However, for the former case, H_{ASSIGNED} should be “approximately” equal to the enthalpy of H₂ at 298.15 K and 0.1 MPA plus the liquid enthalpy of H₂ at 0.1 MPA. The default reference setting of REFPROP does not yield this condition because the liquid enthalpy of H₂ at 0.1 MPA is “almost” zero, (see Table 4). A new relative enthalpy value, at 298.15 K and 0.1 MPA, needs to be input (see Table 5). A new reference state for entropy, at 298.15 K and 0.1 MPA, also needs to be input. This value coincides with the value output by CEA (see Table 6).

**Table A.4: REFPROP Output of H₂ Properties [Ref 5]
Default Reference Setting**

TEMPERATURE K (SATURATED)	PRESSURE MPA	LIQUID DENSITY kg/m ³	VAPOR DENSITY kg/m ³	LIQUID ENTHALPY KJ/kg K	VAPOR ENTHALPY KJ/kg	LIQUID ENTROPY KJ/kg/K	VAPOR ENTROPY KJ/kg/K
20.27	0.1	70.805	1.3368	-0.073542	445.40	-0.0034731	21.974

TEMPERATURE K	PRESSURE MPA	DENSITY kg/m ³	ENTHALPY KJ/kg	ENTROPY KJ/kg/K
298.15	0.1	0.081274	3929.6	53.436

**Table A.5: REFPROP Output of H₂ Properties [Ref 5]
Enthalpy Reference State = 4201 KJ/kg at 298.15 K and 0.1 MPA**

TEMPERATURE K (SATURATED)	PRESSURE MPA	LIQUID DENSITY kg/m ³	VAPOR DENSITY kg/m ³	LIQUID ENTHALPY KJ/kg K	VAPOR ENTHALPY KJ/kg	LIQUID ENTROPY KJ/kg/K	VAPOR ENTROPY KJ/kg/K
20.27	0.1	70.8	1.337	271.2	716.7	11.39	33.36

TEMPERATURE K	PRESSURE MPA	DENSITY kg/m ³	ENTHALPY KJ/kg	ENTROPY KJ/kg/K
298.15	0.1	0.08127	4201.0	64.83

Table A.6: CEA Output of H₂ Properties [Ref 5]

THERMODYNAMIC EQUILIBRIUM PROPERTIES AT ASSIGNED
TEMPERATURE AND PRESSURE

CHEMICAL FORMULA	WT FRACTION	ENERGY KJ/KG-MOL	STATE DEG K	TEMP
FUEL H 2.00000		1.000000	0.000	G 298.15
O/F = 0.0000	PERCENT FUEL = 100.0000	EQUIVALENCE RATIO = 1.0000	PHI = 0.0000	

THERMODYNAMIC PROPERTIES

P, MPA	0.10002
T, DEG	298.15
RHO, KG/CU M	8.1337-2
H, KJ/KG	1.1794
U, KJ/KG	-1228.54
G, KJ/KG	-19327.1
S, KJ/(KG)(K)	64.8272

M, MOL WT	2.016
(DLV/DLP)T	-1.00000
(DLV/DLT)P	1.0000
CP, KJ/(KG)(K)	14.3091
GAMMA (S)	1.4050
SON VEL,M/SEC	1314.4

TRANSPORT PROPERTIES (GASES ONLY)
CONDUCTIVITY IN UNITS OF MILLIWATTS/(CM)(K)

VISC,MILLIPOISE 0.08915

WITH EQUILIBRIUM REACTIONS

CP, KJ/(KG)(K)	14.3097
CONDUCTIVITY	1.8274
PRANDTL NUMBER	0.6981

WITH FROZEN REACTIONS

CP, KJ/(KG)(K)	14.3097
CONDUCTIVITY	1.8274
PRANDTL NUMBER	0.6981

MOLE FRACTIONS

H2	1.00000
----	---------

Appendix B: Calculation of Droplet Inlet Velocity from the Condenser Spray Bar

For an RL-10 engine test run in the B2 facility, the total flow rate injected through the condenser spray bar is:

$$\text{Eq. B.1} \quad \dot{m}_{\text{SB}} = 220000 \text{ [gal/min]} = 13878 \text{ [kg/s]}$$

The number of spray nozzles is:

$$\text{Eq. B.2} \quad N_{\text{noz}} = 694$$

Therefore the flow rate per nozzle is:

$$\text{Eq. B.2} \quad \dot{m}_{\text{noz}} = 19.997 \text{ [kg/s]}$$

The nozzle exit radius is:

$$\text{Eq. B.4} \quad R_{\text{noz}} = 0.077458 \text{ [ft]} = 0.02361 \text{ [m]}$$

Therefore the cross sectional area of a nozzle is:

$$\text{Eq. B.5} \quad A_{\text{cnoz}} = \pi (0.02361)^2 = 0.00175 \text{ [m}^2\text{]}$$

The velocity of the droplet exiting the nozzle is:

$$\text{Eq. B.6} \quad V_{\text{noz}} = \frac{\dot{m}_{\text{noz}}}{\rho_{\text{SB}} A_{\text{cnoz}}} = 11.427 \text{ [m/s]} = 37.5 \text{ [ft/s]}$$

Appendix C: Abbreviations and Acronyms

ANSI	
ASCI	
B2	Spacecraft Propulsion Research Facility
CEA	Chemical Equilibrium with Applications code
CFD	Computational Fluid Dynamics
FORTTRAN	
ft	feet
ft/sec	feet per second
gal/min	gallons per minute
H ₂	hydrogen
H ₂ O	water
ID	Inner Diameter
J/kg/K	Joules per kilogram per degree Kelvin
K	Kelvin
kg/m ³	kilograms per cubic meter
kg/s	kilograms per second
KJ/kg	Kilojoules per kilogram
l/m/kg	liters per meter per kilogram
m	meters
m ²	square meters
m/s	meters per second
MPA	Mega Pascal
MSC Patran	
NASA	National Aeronautics and Space Administration
NIST	
OD	Outer Diameter
Pa	Pascal
REFPROP	Reference Fluid Thermodynamic and Transport Properties
sec	seconds
SMD	Sauter Mean Diameter
SINDA/FLUINT	FLUINT is the fluid systems analyzer, SINDA is the thermal analyzer
W	watts

Appendix D: Obtaining and Running the Model

SINDA/FLUINT 5.3 is very important. There are some double precision conversion issues at the moment.

Appendix E: Nomenclature

k	Thermal conductivity	[W/m/K]
g	Gravity	[m/s ²]
h	Heat transfer coefficient	[W/m ² /K]
$h_{\text{conv_HTUDIF}}$	Heat transfer coefficient for SINDA/FLUINT subroutine HTUDIF	[W/m ² /K]
h_{fg}	Heat of vaporization	[J/kg/K]
h_{eff}	Effective heat transfer coefficient between droplet surface and rocket exhaust duct flow saturation condition	[W/m ² /K]
h'_{fg}	Modified heat of vaporization to account for subcooling	[J/kg/K]
h_{film}	Film boiling heat transfer coefficient	[W/m ² /K]
h_{quench}	Total quench heat transfer coefficient	[W/m ² /K]
j	Diffusion mass flux rate	[kg/s/m ²]
m	Mass	[kg]
\dot{m}	Mass flow rate	[kg/s]
\dot{m}_{water}	Quench water mass flow rate	[kg/s]
"		
m	Mass flux rate	[kg/s/m ²]
r	Droplet radius	[m]
t	Time	[s]
x	Mass fraction	
Ac	Cross-sectional area	[m ²]
As	Surface area	[m ²]
CD	Drag coefficient	
CF	Correction factor for evaporation mass flow rate	
Cp	Specific heat	[J/kg/K]
D	Diameter	[m]
Do	Outer diameter	[m]
D_{wh}	Diffusion coefficient of water and hydrogen	[m ² /s]
F	Friction factor	
FC	SINDA/FLUINT FC factor	[1/m/kg]
FD	Drag force	
F_G	Body force	
G	Thermal conductor	[W/K]
H	Enthalpy	[W/K]
H_{duct}	Enthalpy of shocked rocket exhaust duct flow	[J/kg]
H_{quench}	Enthalpy of shocked rocket exhaust	[J/kg]

	duct flow with quench cooling water	
H_{water}	Enthalpy of quench cooling water duct flow	[J/kg]
H_{CEA}	Enthalpy output from CEA	[KJ/kg]
H_{REFPROP}	Enthalpy output from REFPROP	[KJ/kg]
$H_{\text{REFPROP_satvap_298}}$	Saturated vapor enthalpy at 298.15 K output from REFPROP	[KJ/kg]
Ja	Jakob number	
L	Length	[m]
N_{noz}	Number of nozzles in spray bar	
N_{drop}	Number of droplets in a stratified tank	
$N_{\text{drop}_{\text{in}}}$	Number of droplets entering a stratified tank	
Nu	Nusselt Number	
P_{tot}	Total Pressure	[Pa]
Pr	Prandtl number	
Q	Heat rate	[W]
QL	Heat rate applied to SINDA/FLUINT tank	[W]
R	Radius	[m]
Re	Reynolds number	
S_{CEA}	Entropy output from CEA	[KJ/kg/K]
S_{REFPROP}	Entropy output from REFPROP	[KJ/kg/K]
$S_{\text{REFPROP_satliq_298}}$	Saturated liquid entropy at 298.15 K	[KJ/kg/K]
T_o	Outer wall temperature	[K]
T_{stat}	Static temperature	[K]
T_{rec}	Recovery temperature	[K]
T_{ref}	Reference temperature	[K]
T_{stag}	Stagnation temperature	[K]
T_{wall}	Wall temperature	[K]
T_{d}^n	Temperature of the n^{th} node of a characteristic droplet	[K]
$T_{\text{in}_{\text{d}}}^n$	Temperature of the n^{th} node of a characteristic droplet entering a stratified tank	[K]
$T_{\text{old}_{\text{d}}}^n$	Temperature of the n^{th} node of a characteristic droplet in a stratified tank at the previous time step	[K]
V	Velocity	[m/s]
$V_{\text{in}_{\text{d}}}$	Velocity of characteristic a droplet entering a stratified tank	[m/s]
$V_{\text{old}_{\text{d}}}$	Velocity of characteristic a droplet in a stratified tank at the previous time step	[m/s]
V_{rel}	Relative Velocity	[m/s]
XL	Quality of a stratified tank	
ρ	Density	[kg/m ³]

μ		Viscosity	[kg/m/s]
-------	--	-----------	----------

Subscripts

cond		Condensation	
conv		Sensible heat transport and transfer via convection and conduction	
duct		Rocket exhaust duct	
d		Droplet	
evap		Evaporation	
h		Hydrogen	
i		Interface between droplet condensate layer and diffusion layer (saturation conditions of droplet)	
n		Droplet thermal node number	
noz		Spray bar nozzle	
s		Droplet surface	
sat		Saturation	
satd		Droplet saturation condition	
satv		Saturated vapor	
sat ∞		Rocket exhaust duct flow saturation condition	
v		Vapor	
walld		Droplet wall	
w		Water	
D		Duct	
SB		Spray bar	
ℓ		Liquid	
∞		Exhaust duct flow	

Constants

g	9.81	Gravity	[m/s ²]
Π	3.1415		
H _{ASSIGNED}	4470.0	Assigned enthalpy of liquid/vapor H ₂ in CEA	[KJ/kg]
H _f	-13423.647	Enthalpy of formation of H ₂ O vapor at 298.15 K and 0.1 MPA	[KJ/kg]
S _f	3.882	Absolute Entropy of H ₂ O liquid at 298.15 K and 0.1 MPA	[KJ/kg/K]
ρ_{SB}	1000.0	Liquid water density	[kg/m ³]

References

1. Chung, J.N., Ayyaswamy, P.S., "Laminar Condensation Heat and Mass Transfer in the Vicinity of the Forward Stagnation Point of a Spherical Droplet Translating in a Ternary Mixture: Numerical and Asymptotic Solutions", *Int. J. Heat Mass Transfer*, Vol 21, pp 1309-1324, Pergamon Press Ltd., 1978.
2. Eckert, E. R. G., "Survey on Heat Transfer at High Speeds," *Aeronaut. Res. Lab. Rep. 189*, Office of Aerospace Research, Wright Patterson Air Force Base, Ohio, 1961.
3. Chapman, Alan J., *Heat Transfer*, 4th ed., Macmillan Publishing Co., New York, 1984.
4. C&R Technologies, *SINDA/FLUINT General Purpose Network Thermal/Fluid Analyzer User's Manual*, Version 4.8, April 2006.
5. Lemmon, E.W., McLinden, M. O., Huber, M.L., "Reference Fluid Thermodynamic and Transport Properties", *NIST Standard Reference Database 23*, Version 7.0, Physical and Chemical Properties Division, US Secretary of Commerce on behalf of the United States of America, 2002.
6. McBride, Bonnie J., Gordon, Sanford, "Computer Program for Calculation of Complex Chemical Equilibrium Compositions and Applications, II. Users Manual and Program Description, *NASA Reference Publication 1311*, June 1996.
7. White, Larry C., "External Flow Film Boiling", *Handbook of Phase Change: Boiling and Condensation*, Kandikar, Satish G., Shoji, Masahiro, Dhir, Vijay K., Taylor & Francis, Philadelphia, Pa, 1999.
8. ANSYS CFX Solver, Release 10.0 User's Manual: Theory Multiphase Flow, SAS IP, Inc., 2004.
9. Incropera, Frank P., Dewitt, David P., *Fundamental of Heat and Mass Transfer*, John Wiley & Sons, Inc., 1981.
10. Collier, John G., Thome, John R., *Convective Boiling and Condensation*, 3rd ed., Clarendon Press, Oxford, 1996.
11. Lefebvre, Arthur, *Atomization and Sprays (Combustion: An International Series)*, Taylor & Francis, 1989.